Inorganic Chemistry

Article

pubs.acs.org/IC

Activation of the Hg−C Bond of Methylmercury by [S_2]-Donor Ligands

Ramesh Karri, Mainak Banerjee, Ashish Chalana, Kunal Kumar Jha, and Gouriprasanna Roy*

Department of Chemistry, School of Natural Sciences, Shiv Nadar University, NH91, Dadri, Gautam Buddha Nagar, Uttar Pradesh 201314, India

Supporting Information

ABSTRACT: Here we report that [S_2]-donor ligands Bmm^{OH}, Bmm^{Me}, and Bme^{Me} bind rapidly and reversibly to the mercury centers of organomercurials, RHgX, and facilitate the cleavage of Hg−C bonds of RHgX to produce stable tetracoordinated Hg(II) complexes and R_2Hg. Significantly, the rate of cleavage of Hg−C bonds depends critically on the X group of RHgX (X = BF_4^-, Cl^-, I^-) and the [S_2]-donor ligands used to induce the Hg−C bonds. For instance, the initial rate of cleavage of the Hg−C bond of MeHgI induced by Bme^{Me} is almost 2-fold higher than the initial rate obtained by Bmm^{OH} or Bmm^{Me}, indicating that the spacer between the two imidazole rings of [S_2]-donor ligands plays a significant role here in the cleavage of Hg−C bonds. Surprisingly, we noticed that the initial rate of cleavage of the Hg−C bond of MeHgI induced by Bme^{Me} (or Bmm^{Me}) is almost 10-fold and 100-fold faster than the cleavage of Hg−C bonds of MeHgCl and [MeHg]BF_4 respectively, under identical reaction conditions, suggesting that the Hg−C bond of [MeHg]BF_4 is highly inert at room temperature (21 °C). We also show here that the nature of the final stable cleaved products, i.e. Hg(II) complexes, depends on the X group of RHgX and the [S_2]-donor ligands. For instance, the reaction of Bmm^{Me} with MeHgCl (1:1 molar ratio) afforded the formation of the 16-membered metallacyclic dinuclear mercury compound $(Bmm^{Me})_2Hg_2Cl_4$, in which the two Cl atoms are located inside the ring, whereas due to the large size of the I atom, a similar reaction with MeHgI yielded polymeric $[(Bmm^{Me})_2HgI_2]_m\cdot(MeHgI)_n$. However, the treatment of Bmm^{Me} with ionic [RHg]BF_4 led to the formation of the tetrathione-coordinated mononuclear mercury compound $[(Bmm^{Me})_2Hg](BF_4)_2$, where BF_4^- serves as a counteranion.

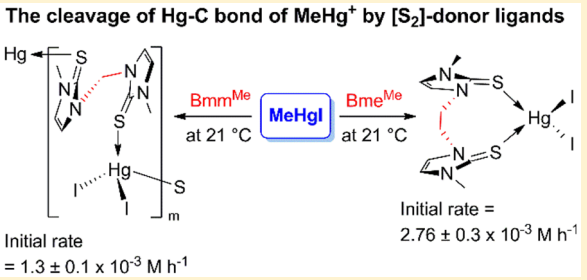

INTRODUCTION

Organomercurials (often referred to as RHg^+), including methylmercury ($MeHg^+$), are among the most toxic compounds to humans and animals. $MeHg^+$ exists in the environment in various chemical forms, including MeHgOH, MeHgCl, and MeHgI. The toxicity of $MeHg^+$ is mainly attributed to its lipophilicity and strong binding affinity toward thiols present in proteins.[1−5] On the other hand, due to its structural similarity with the natural amino acid L-methionine, the L-cysteine-conjugated $MeHg^+$ (MeHgCys) acts as a substrate for the membrane transporter L-type large neutral amino acid transporter 1 (LAT1), which is expressed in many tissues and actively facilitates the transportation of large neutral amino acids including L-methionine and MeHgCys in multiple tissues, including brain.[4a,6,7] Thus, the ability of $MeHg^+$ to interact with L-cysteine is critical for its ability to gain intracellular access and exert its cytotoxicity. A report suggests that the toxicological implications associated with the ingestion of $MeHg^+$ may differ according to its chemical form.[8] Murakami and co-workers showed that the pharmacokinetic properties such as the mechanism of membrane transport and volume of distribution are quite different between MeHgCl and MeHgCys.[9] Moreover, MeHgI is an another organic pollutant present in the environment, and it has also been detected in the egg samples of California Black skimmers collected from the remnant coastal wetlands.[10,11] The binding affinity of Hg^{2+} for Cl^- or I^- is very high, and thus, the Hg−Cl or Hg−I bond in MeHgX may remain intact in aqueous solution in the absence of a strongly electron donating ligand.[8a,12] Thus, a clear understanding of the role of X (X = Cl^-, I^-) on the cleavage of Hg−C bonds of MeHgX is of great importance.

On the other hand, several bacteria are resistant to $MeHg^+$ due to the presence of a *mer* operon that codes for two enzymes: namely, organomercurial lyase (MerB) and mercurial reductase (MerA). The enzyme MerB first cleaves the Hg−C bond of $MeHg^+$ to form Hg(II) and subsequently transfers Hg(II) to another enzyme MerA, which reduces it to elemental Hg(0).[13−15] The active site of MerB consists of a catalytic triad of two cysteine residues (Cys) and either an aspartic acid (Asp) or a serine (Ser) residue.[14−17] Although the two Cys residues are conserved in the active sites of all known variants of MerB (total 65 complete protein sequences of organomercurial lyases are identified as of January 2010, UniProtKB database), four variants of organomercurial lyases (*Bacillus megaterium* MerB2, *Bacillus subtillis* MerB2, *Bacillus* sp. (RC607) MerB2, and

Received: April 27, 2017

DOI: 10.1021/acs.inorgchem.7b01048
Inorg. Chem. XXXX, XXX, XXX−XXX

Clostridium butyricum MerB2) carry a Ser residue instead of Asp in their catalytic triad. Significantly, recent studies showed that the presence of a Ser residue in the active site substantially reduces the catalytic activity as well as the substrate specificity of these four MerB2 variants.[18−20] However, the mechanism by which these serine-containing organomercurial lyases (MerB2) cleave the Hg−C bonds of organomercurials has not been studied yet. In this context, therefore, it is beneficial to develop chemistry between [S_2]-donor ligands with various $MeHg^+$ compounds (such as ionic $[MeHg]BF_4$, MeHgCl, and MeHgI) which may help in understanding the mechanism of detoxification of $MeHg^+$ by microorganisms. In this study, we have employed the three imidazole-based [S_2]-donor ligands Bmm^{OH}, Bmm^{Me}, and Bme^{Me} with different N substitutions and spacers between the two imidazole rings (Figure 1), to

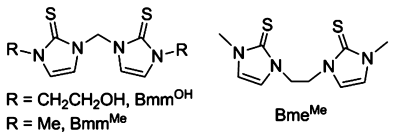

Figure 1. Chemical structures of [S_2]-donor ligands.

investigate their potential in the cleavage of inert Hg−C bonds of various organomercurials RHgX (where R = Me, Et, Ph and X = BF_4^-, Cl^-, I^-) at physiological temperature (37 °C).

RESULTS AND DISCUSSION

The [S_2]-donor ligands Bmm^{OH}, Bmm^{Me}, and Bme^{Me} were synthesized by in situ generation of reactive carbenes from various bis-imidazolium salts by following the literature procedures.[21,22] Detailed synthetic procedures are mentioned in the Supporting Information. Although the cleavage of Hg−C bonds of $MeHg^+$ by the [S_3]-donor ligand tris(2-mercapto-1-R-imidazolyl)hydroborato [Tm^R],[23] the [P_3]-donor ligand N-$(CH_2CH_2PPh_2)_3$,[24] and other ligands,[25] in the absence or presence of proton donor (thiol or CF_3CO_2H), has been reported previously in the literature, the cleavage of Hg−C bonds of organomercurials by any [S_2]-donor ligands and the development of coordination chemistry between them have not been studied earlier. In this study, we use Bmm^{OH}, Bmm^{Me}, or Bme^{Me} to understand the cleavage of Hg−C bonds of RHgX. The treatment of Bmm^{OH} with 1 equiv of $[RHg]BF_4$ (R = Ph, Et, Me) at 21 °C led to the formation of the corresponding 1:1 RHg-conjugated complexes $[(Bmm^{OH})HgR]BF_4$ (Figure 2). The NMR spectroscopy studies of the reaction solutions of Bmm^{OH} and $[RHg]BF_4$ have provided very useful information about coordination of S atoms of Bmm^{OH} to the mercury centers of $[RHg]BF_4$. Interestingly, the resulting solution of Bmm^{OH} and $[MeHg]BF_4$ in a 1:1 molar ratio showed only a single set of signals of $[(Bmm^{OH})HgMe]BF_4$ in ^1H NMR spectroscopy, as shown in Figure 2b and the Supporting Information. The signal for the methyl group of −HgMe appeared at 0.71 ppm in DMSO-d_6, which was in a slightly different position in comparison to that for $[MeHg]BF_4$ alone (at 0.79 ppm in DMSO-d_6) (Figures S20 and S21 in the Supporting Information). Surprisingly, the addition of more Bmm^{OH} to the above solution ($[Bmm^{OH}]/[MeHg^+]$ = 2 or more) resulted in only a single set of signals. In addition, the observation of two signals for four olefinic hydrogen atoms (or (imidazole)CH) of two imidazole rings of Bmm^{OH} in ^1H NMR

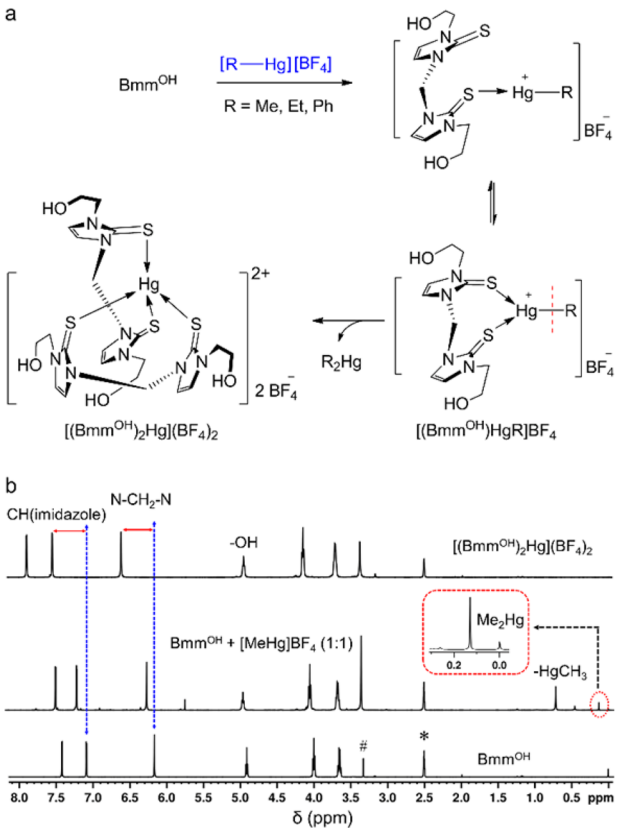

Figure 2. (a) Synthetic route for the cleavage of Hg−C bonds of $[RHg][BF_4]$ by Bmm^{OH}. (b) ^1H NMR spectra, in DMSO-d_6, of Bmm^{OH}, a mixture of Bmm^{OH} and $[MeHg]BF_4$, and $[(Bmm^{OH})_2Hg](BF_4)_2$ (isolated), also showing the formation of Me_2Hg (*, DMSO-d_6; #, H_2O in DMSO-d_6).

spectroscopy suggests that both S atoms of Bmm^{OH} are involved in coordination to the mercury center of $[MeHg]BF_4$ in solution (two chemically equivalent imidazole rings). These observations suggest that, in solution, all of the Bmm^{OH} molecules are involved in interacting with the mercury center of $[MeHg]BF_4$ through S atoms and this interaction is rapid, is faster than the NMR time scale, and is reversible in nature (fluxional behavior prevents the identification of the excess free ligands in solution).[26] A similar phenomenon was also noticed at low temperature (−30 °C in $CDCl_3$), indicating that this exchange process is highly facile even at low temperature. Accordingly, the ^{199}Hg NMR signal of $[MeHg]BF_4$, in DMSO-d_6, shifted from −1086 to −712 ppm after addition of 1 equiv of Bmm^{OH}, indicating the coordination of S atoms of Bmm^{OH} to the mercury center of $[MeHg]BF_4$ (Figure S46 in the Supporting Information). The formation of $[(Bmm^{OH})HgMe]^+$ in solution was detected by mass spectrometry (m/z for $[(Bmm^{OH})HgMe]^+$ 517.0644). However, when the reaction was continued at high temperature (37 °C) for 7 days, the cleavage of the Hg−C bond of $[(Bmm^{OH})HgMe]^+$ and subsequently the formation of the stable tetracoordinated mononuclear mercury compound $[(Bmm^{OH})_2Hg](BF_4)_2$ (m/z for $[(Bmm^{OH})_2Hg]^{2+}$ 401.0538) and volatile dimethylmercury (Me_2Hg) were observed (Figure 3). The ^{199}Hg NMR signals for $[(Bmm^{OH})_2Hg]^{2+}$ and Me_2Hg appeared at −443 and −113 ppm, respectively, in DMSO-d_6 (Figure 3c).[27]

Recently we have shown that N-substituted imidazole and benzimidazole-based thiones and selones having an N−

DOI: 10.1021/acs.inorgchem.7b01048
Inorg. Chem. XXXX, XXX, XXX−XXX

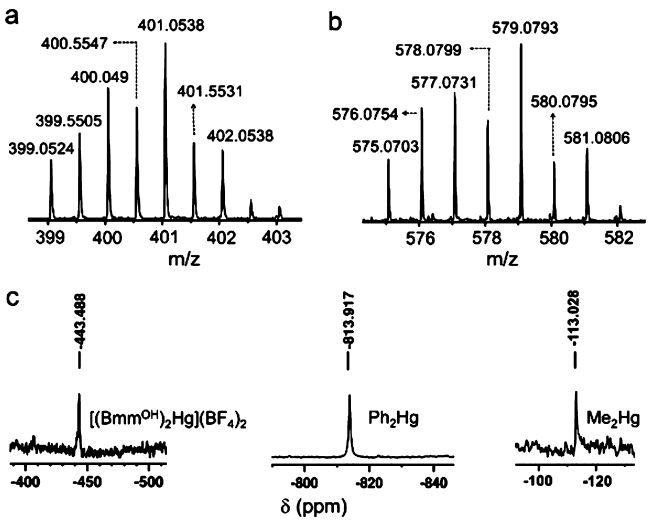

Figure 3. HRMS of $[(Bmm^{OH})_2Hg]^{2+}$ (a) and $[(Bmm^{OH})HgPh]^{+}$ (b) and ^{199}Hg NMR spectra of $[(Bmm^{OH})_2Hg](BF_4)_2$, Ph_2Hg, and Me_2Hg in DMSO-d_6 (c).

CH_2CH_2OH substituent are remarkably effective in detoxifying various organomercurials by converting them into less toxic insoluble HgS(s) and HgSe(s) nanoparticles in the presence of 1 equiv of strong or weak base.[28] However, in this case the addition of 1 equiv of KOH to the reaction mixtures of Bmm^{OH} plus $[RHg]BF_4$ failed to produce HgS(s) nanoparticles at 37 °C. Interestingly, the ^1H NMR spectrum of the cleaved product $[(Bmm^{OH})_2Hg](BF_4)_2$ showed that the −OH groups of Bmm^{OH} remained free in solution and were not involved in coordination to the mercury center (Figure 2b). The large downfield chemical shift of the bridging methylene group (N−CH_2−N) (0.45 ppm) and the olefinic H atoms of imidazole rings (0.46 ppm) was observed in $[(Bmm^{OH})_2Hg](BF_4)_2$ in comparison to those in the free ligand Bmm^{OH}. Likewise, the ^{199}Hg NMR of a reaction mixture containing Bmm^{OH} and $[PhHg]BF_4$ in 1:1 molar ratio showed a signal at −1154 ppm which was shifted almost 225 ppm downfield in comparison to that observed for free $[PhHg]BF_4$ at −1379 ppm, indicating a strong coordination between the S atoms of Bmm^{OH} to the mercury center of $[PhHg]BF_4$. However, similar to the case of Bmm^{OH} and $[MeHg]BF_4$, as the reaction between Bmm^{OH} and $[PhHg]BF_4$ was allowed to proceed for 48 h at 37 °C, the formation of cleaved product $[(Bmm^{OH})HgPh]^{+}$ and diphenylmercury (Ph_2Hg) were observed. The monopositive $[(Bmm^{OH})HgPh]^{+}$ (m/z 579.0793) and the dipositive $[(Bmm^{OH})_2Hg]^{2+}$ (m/z 401.0538) species were detected by mass spectrometry (Figure 3). Ph_2Hg was extracted with a nonpolar solvent (hexane) and characterized by NMR spectroscopy. The ^{199}Hg NMR of Ph_2Hg (0.1 M) was detected at −814 ppm in DMSO-d_6.[29]

Although the coordination complexes of Bmm^{Me} and Bme^{Me} with other metal ions, except mercury, have been reported in the literature,[22,30] cleavage of the Hg−C bonds of organomercurials by Bmm^{Me} or Bme^{Me} has not been studied yet. Rabinovich et al. has reported a coordination complex of Hg(II) with the $[S_2]$-donor ligand bis(mercaptoimidazolyl)-borate (Bm^R)[31] but no coordination complex of Bmm^{Me} or Bme^{Me} with mercury has been reported in the literature. To investigate the effect of N substitution on the cleavage of the Hg−C bond, we have treated Bmm^{Me} with $[RHg]BF_4$ (R = Ph, Et, Me) under identical reaction conditions to produce the 1:1 RHg-conjugated complexes $[(Bmm^{Me})HgR]BF_4$ (m/z (for M^+) 519.0627 when R = Ph; m/z 471.0633 when R = Et; m/z 457.0467 when R = Me) (Figure 4a and Figured S7−S9 in the

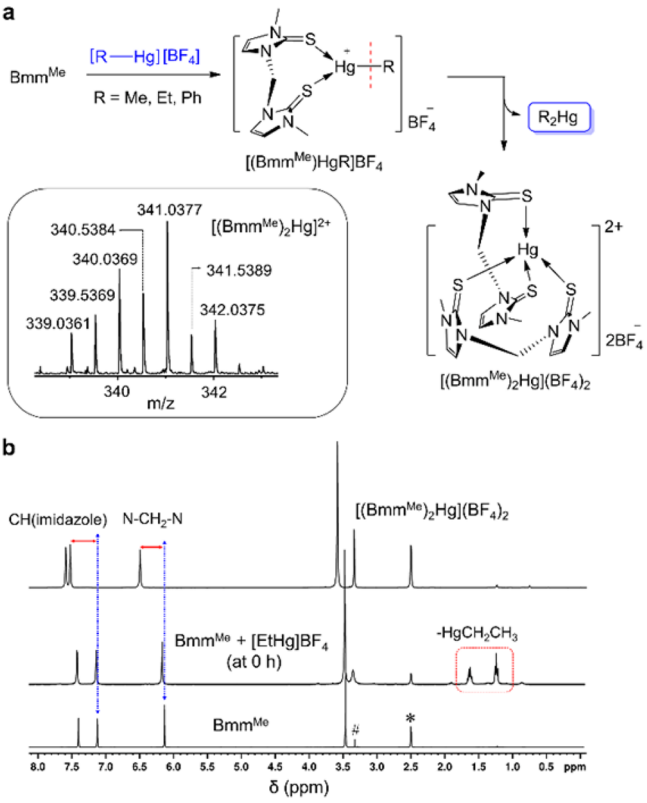

Figure 4. (a) Synthetic route for the synthesis of $[(Bmm^{Me})_2Hg](BF_4)_2$ and the mass spectrum of $[(Bmm^{Me})_2Hg]^{2+}$. (b) ^1H NMR spectra, in DMSO-d_6, of Bmm^{Me}, a mixture of Bmm^{Me} and $[EtHg]BF_4$, and isolated $[(Bmm^{Me})_2Hg](BF_4)_2$ (*, DMSO-d_6; #, H_2O in DMSO-d_6).

Supporting Information). The ^{199}Hg NMR signals of $[(Bmm^{Me})HgR]BF_4$ were observed at −1154 ppm (R = Ph), −873 ppm (R = Et), and −750 ppm (R = Me), respectively. However, at high temperature (37 °C), the 1:1 complexes $[(Bmm^{Me})HgR]BF_4$ gradually degraded to the stable tetracoordinated mononuclear Hg(II) complex $[(Bmm^{Me})_2Hg](BF_4)_2$, where a BF_4^- ion serves as the counterion (m/z for M^{2+} 341.0377; ^{199}Hg NMR signal appeared at −719 ppm), and R_2Hg in solution. ^1H NMR of the isolated cleaved product $[(Bmm^{Me})_2Hg](BF_4)_2$ showed large downfield chemical shifts of the N−CH_2−N group (0.36 ppm) and the olefinic hydrogen atoms of imidazole rings (0.4 ppm) in solution in comparison to those in free Bmm^{Me} molecule (Figure 4b).

The single-crystal X-ray structure analysis of $[(Bmm^{Me})_2Hg](BF_4)_2$ showed that both S atoms of Bmm^{Me} are indeed coordinated to the same Hg(II) atom in a rather unsymmetrical manner (Figure 5). The S1 (or S1′) atom of Bmm^{Me} is coordinated very strongly to the Hg(II) atom (d_{Hg-S1} = 2.465 Å, $d_{Hg-S1'}$ = 2.458 Å), whereas the S2 atom (or S2′) of the same Bmm^{Me} molecular unit is coordinated weakly to the same mercury center (d_{Hg-S2} = 2.651 Å, $d_{Hg-S2'}$ = 2.613 Å). As a consequence, the C−S bond length between the C2A and S1 atoms of $[(Bmm^{Me})_2Hg](BF_4)_2$ (d_{C2A-S1} = 1.714 Å; $d_{C2A'-S1'}$ = 1.720 Å) is slightly longer than the other C−S bond length of the same Bmm^{Me} molecular unit, i.e. between the C2B and S2

DOI: 10.1021/acs.inorgchem.7b01048
Inorg. Chem. XXXX, XXX, XXX−XXX

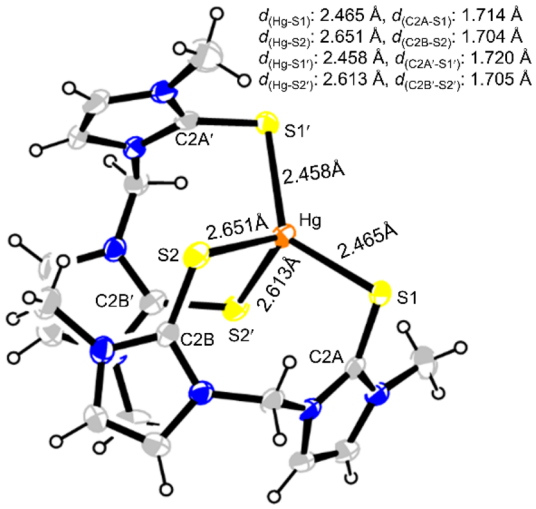

Figure 5. ORTEP diagram of $[(Bmm^{Me})_2Hg](BF_4)_2$. Counterions are omitted for clarity (CCDC1534008).

atoms (d_{C2B-S2} = 1.704 Å; $d_{C2B'-S2'}$ = 1.705 Å), and significantly longer than the C−S bond length in the free Bmm^{Me} molecule (d_{C-S} = 1.680 Å). The bond angle among the S1, Hg, and S1′ atoms is wider (S1−Hg−S1′ = 132.65°) in comparison to the bond angle among S2, Hg, and S2′ atoms (S2−Hg−S2′ = 102.46°), which is quite expected considering the strong coordination of S1 and S1′ atoms to the Hg(II) atom.

From X-ray crystal structure analysis and quantum mechanical calculations (DFT) of $[S_2]$-donor ligands it is quite evident that the structures of free Bmm^{OH}, Bmm^{Me}, and Bme^{Me} primarily exist in zwitterionic form with negative charge on the S atoms and the delocalized positive charge on the imidazole ring (Table 2, Figure S5 in the Supporting Information).[30] Moreover, because of the coordination to the Hg(II) center by p-type sulfur lone pairs, the overall positive charge on the imidazole rings of $[(Bmm^{Me})_2Hg](BF_4)_2$ is expected to increase further in comparison to that observed in free ligands. Crystal packing arrangements of $[(Bmm^{Me})_2Hg](BF_4)_2$ in the solid state showed the presence of multiple nonbonded intermolecular C−H···F hydrogen-bonding interactions (Figure 6). The olefinic H atoms (or (imidazole)CH atom), the H atoms of the N−Me group, and the H atoms of the N−CH_2−N group are engaged in strong nonbonded intermolecular C−H···F hydrogen-bonding interactions ($d_{CH\cdots F}$ = 2.279−2.628 Å) with the F atoms of BF_4^- anions in the solid state.

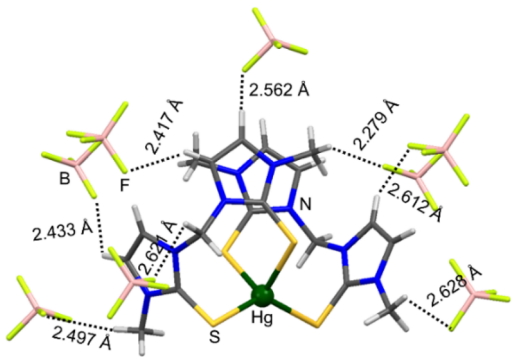

Figure 6. Crystal packing diagram of $[(Bmm^{Me})_2Hg](BF_4)_2$ showing the nonbonded intermolecular C−H···F hydrogen-bonding interactions with BF_4^- anions (image drawn with Mercury 3.8 software).

To understand the effect of imidazole-based $[S_2]$-donor ligands on RHgCl, we have treated Bmm^{Me} with RHgCl (R = Me, Et, Ph), in a 1:1 molar ratio, which afforded the immediate formation of the 1:1 adduct $(Bmm^{Me})HgRCl$ (Figure 7a). The

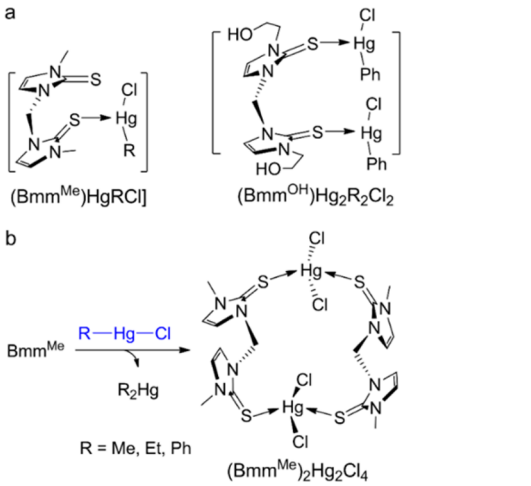

Figure 7. (a) Chemical structures of $(Bmm^{Me})HgRCl$ and (Bmm^{OH})-$Hg_2Ph_2Cl_2$. (b) Formation of $(Bmm^{Me})_2Hg_2Cl_4$ in the reaction of Bmm^{Me} with RHgCl (1:1 molar ratio).

affinity of Cl^- to mercury is very high; therefore, it presumably remains intact with mercury in solution, which is further supported by the isolation and X-ray structure determination of $(Bmm^{OH})Hg_2Ph_2Cl_2$ (CCDC 1534015) from a solution of Bmm^{OH} and PhHgCl, in a 1:2 molar ratio, at low temperature (Supporting Information). The adducts $(Bmm^{Me})HgRCl$, however, were unstable in solution at 37 °C and led to the facile cleavage of the Hg−C bonds and yielded the formation of the stable 16-membered neutral metallacycle $(Bmm^{Me})_2Hg_2Cl_4$ as the end product, in which the two chloride ions are covalently attached with each mercury center (Figure 7b). ^1H NMR spectroscopy was used to monitor the cleavage of Hg−C bonds in the reaction of RHgCl with Bmm^{Me} or Bmm^{OH} (in a 1:1 molar ratio), as illustrated in Figure 8 and the Supporting Information.

During the crystallization process of solutions containing Bmm^{Me} and RHgCl ($[Bmm^{Me}]/[RHgCl]$ = 1) we have isolated two different types of crystals; one was the diamond-shaped crystal $(Bmm^{Me})_2Hg_2Cl_4$, which was always cocrystallized with various solvent molecules (CCDC 1534011, $(Bmm^{Me})_2Hg_2Cl_4$·2ACN; CCDC 1534012, $(Bmm^{Me})_2Hg_2Cl_4$·2DMF), and the other one was needle-shaped crystals of the starting material Bmm^{Me} (Table 3). The X-ray structure determination of the isolated product $(Bmm^{Me})_2Hg_2Cl_4$ showed very interesting structural features (Figure 9). Two sulfur atoms of Bmm^{Me} are coordinated symmetrically and somewhat strongly to the two different mercury centers, leading to the formation of the 16-membered metallacycle $(Bmm^{Me})_2Hg_2Cl_4$. As a result, a significant amount of increase in C−S bond lengths of coordinated Bmm^{Me} in $(Bmm^{Me})_2Hg_2Cl_4$ is observed in comparison to those in free Bmm^{Me}. The lengths of Hg−S and C−S bonds in $(Bmm^{Me})_2Hg_2Cl_4$ are 2.490 and 1.714 Å, respectively. Interestingly, $(Bmm^{Me})_2Hg_2Cl_4$ contains two completely different types of Hg−Cl bonds ($d_{Hg1-Cl1}$ = 2.521 Å, $d_{Hg1-Cl2}$ = 2.655 Å, $d_{Hg2-Cl3}$ = 2.655 Å, $d_{Hg2-Cl4}$ = 2.521 Å).

DOI: 10.1021/acs.inorgchem.7b01048
Inorg. Chem. XXXX, XXX, XXX−XXX

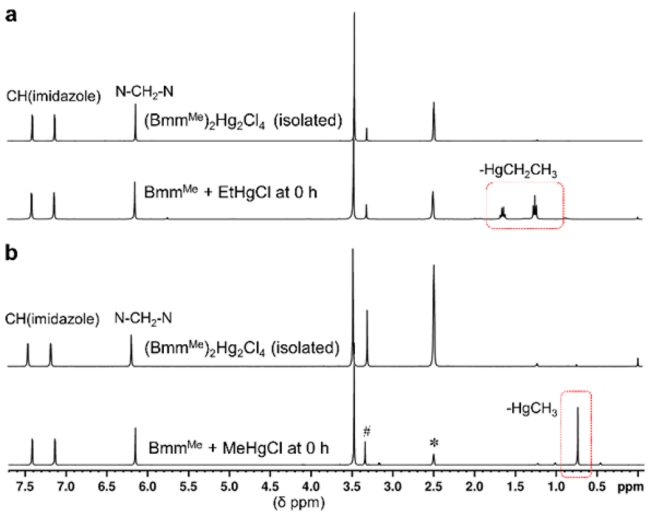

Figure 8. ^{1}H NMR spectra, in DMSO-d_6, of solutions containing Bmm^{Me} and EtHgCl (a), Bmm^{Me} and MeHgCl (b), and isolated (Bmm^{Me})Hg_2Cl_4 (*, DMSO-d_6; #, H_2O in DMSO-d_6).

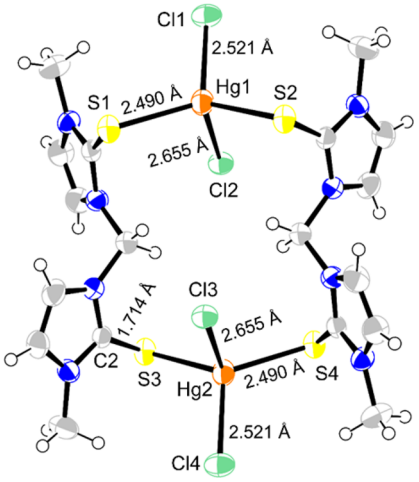

Figure 9. ORTEP diagram of (Bmm^{Me})$_2Hg_2Cl_4$.

The two chlorine atoms Cl1 and Cl4, which are oriented toward the outside of the 16-membered ring, formed shorter Hg−Cl bonds (2.521 Å), whereas the other two Cl atoms, Cl2 and Cl3, which are sandwiched between the two imidazole rings, formed significantly longer Hg−Cl bonds (2.650 Å), as shown in Figure 10.

In view of the fact that the reactions of Bmm^{Me} with $RHgBF_4$ and RHgCl afforded completely two different types of coordination compounds, namely (Bmm^{Me})$_2Hg_2Cl_4$ and

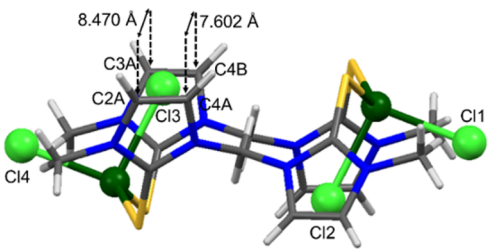

Figure 10. Molecular structure of (Bmm^{Me})$_2Hg_2Cl_4$ showing the orientation of Cl atoms in the molecule.

[(Bmm^{Me})$_2$Hg](BF$_4$)$_2$ respectively, indicating that the anion (BF_4^- or Cl^-) has a significant role in deciding the final products in these reactions, we have investigated the effect of Bmm^{Me} on MeHgI. Treatment of MeHgI with Bmm^{Me} in a 1:1 molar ratio in dichloromethane afforded a white precipitate of the 1:1 complex (Bmm^{Me})HgMeI at room temperature, which was isolated by filtration and characterized thoroughly by various techniques. However, when a solution of this complex (Bmm^{Me})HgMeI in methanol was stirred at high temperature (37 °C), we observed a gradual formation of Me_2Hg and the cleaved product [(Bmm^{Me})HgI_2]$_m$·(MeHgI)$_n$, which was crystallized from methanol (Scheme 1 and Figure 11).

Scheme 1. Synthetic Routes for the Synthesis of [(Bmm^{Me})HgI_2]$_m$·(MeHgI)$_n$ and Bme^{Me}HgI_2

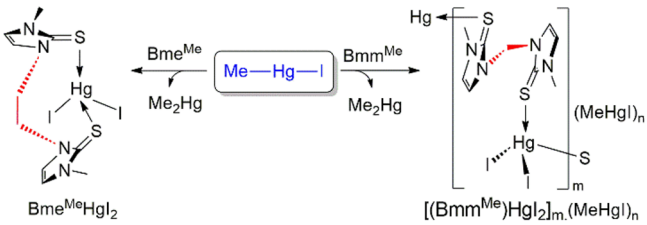

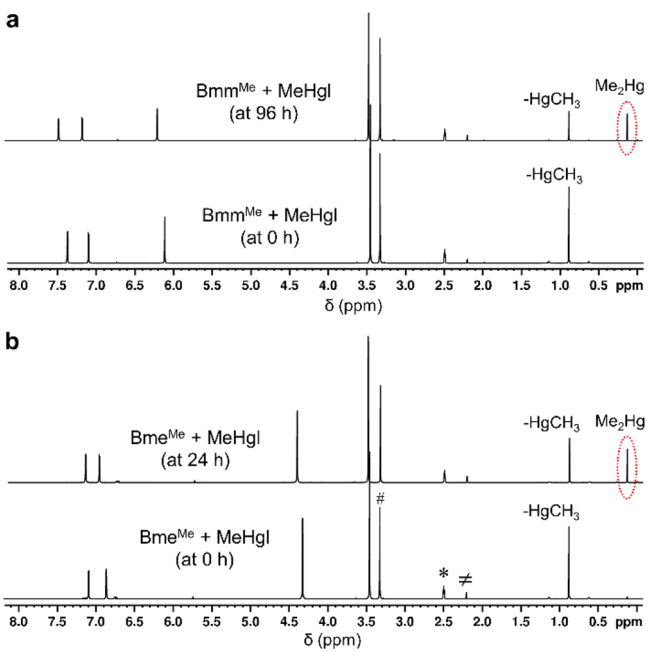

Figure 11. ^{1}H NMR spectra in DMSO-d_6 showing the cleavage of the Hg−C bond of MeHgI by Bmm^{Me} (a) and Bme^{Me} (b), in a 1:1 molar ratio, and the formation of Me_2Hg (*, DMSO-d_6; #, H_2O in DMSO-d_6; ≠, mesitylene; [MeHgI] = 0.1 M).

X-ray analysis of colorless needle-shaped crystals showed the formation of [(Bmm^{Me})HgI_2]$_m$·(MeHgI)$_n$, where MeHgI was cocrystallized with the cleaved product [(Bmm^{Me})HgI_2]$_m$ (m = n, Figure 12; CCDC 1534014). Thus, ^{1}H NMR spectroscopic studies and an X-ray structure analysis have confirmed that the [S_2]-donor ligands can facilitate the cleavage of the Hg−C bond of MeHgI. X-ray structure analysis of [(Bmm^{Me})HgI_2]$_m$·(MeHgI)$_n$ revealed that the two S atoms of Bmm^{Me} interact with the two different mercury centers, resulting in the formation of a polymeric structure, as illustrated in Figures 12 and 13. As both S atoms of the C=S moieties of Bmm^{Me}

DOI: 10.1021/acs.inorgchem.7b01048
Inorg. Chem. XXXX, XXX, XXX−XXX

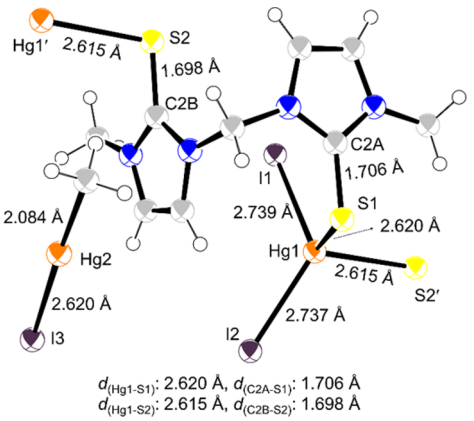

Figure 12. ORTEP diagram of $[(Bmm^{Me})HgI_2]_m \cdot (MeHgI)_n$.

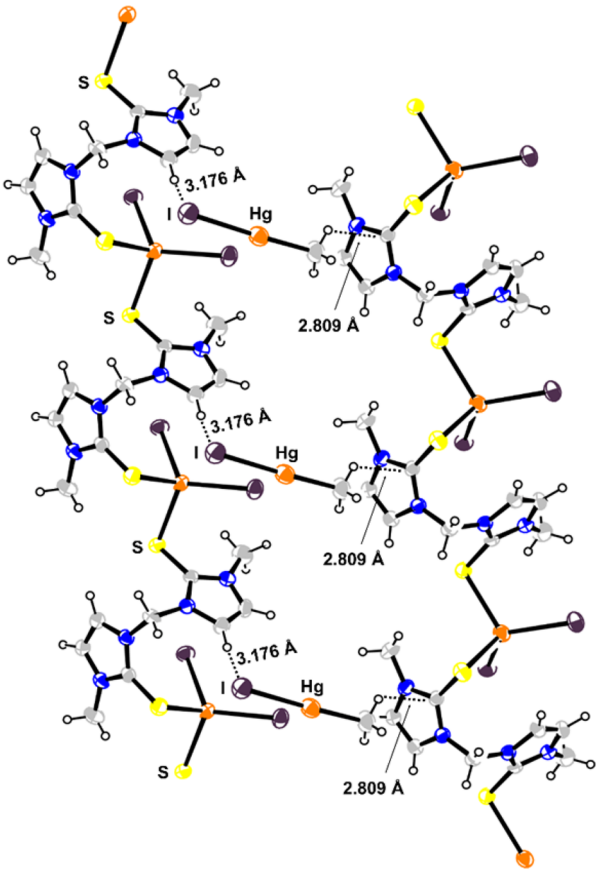

Figure 13. Packing diagram of $[(Bmm^{Me})HgI_2]_m \cdot (MeHgI)_n$.

interacted almost equally with the tetracoordinated Hg(II) atom, the two Hg−S bonds are equal in length (d_{Hg1-S1} = 2.620 Å and $d_{Hg1'-S2}$ = 2.615 Å). Likewise, the corresponding C−S bonds of coordinated Bmm^{Me} are also equally elongated (d_{C2A-S1} = 1.706 Å; d_{C2B-S2} = 1.698 Å) from 1.680 Å in the free Bmm^{Me} molecule. The high affinity of iodide ion for Hg(II) has been confirmed through the presence of two Hg−I bonds in $[(Bmm^{Me})HgI_2]_m$. The two Hg−I bonds in $[(Bmm^{Me})HgI_2]_m \cdot (MeHgI)_n$ are equal in length with an average bond distance of 2.738 Å, which is slightly longer than the Hg−I bond distance (2.62 Å) present in MeHgI that is cocrystallized with the complex. Interestingly, the crystal packing of $[(Bmm^{Me})HgI_2]_m \cdot (MeHgI)_n$ showed that MeHgI molecules formed a bridge between the two parallel 1D linear chains of $[(Bmm^{Me})HgI_2]_m$. The iodine atom of MeHgI involves nonbonded intermolecular C−H···I hydrogen-bonding interactions with the olefinic H atom of the imidazole ring of one chain. On the other hand, the H atom of the methyl group of MeHgI forms a nonbonded interaction with the π electrons of the imidazole ring of the other 1D linear chain of $[(Bmm^{Me})HgI_2]_m$ (Figure 13).

We have studied in detail the cleavage of Hg−C bonds of MeHgX (X = Cl^-, I^-) induced by $[S_2]$-donor ligands Bmm^{OH}, Bmm^{Me}, and Bme^{Me} to understand the role of the X group of MeHgX and the spacer group between the two imidazole rings of $[S_2]$-donor ligands. The cleavage of Hg−C bonds of MeHgX was monitored by ^{1}H NMR spectroscopy, and all experiments were performed at room temperature (21 °C) (for more details see the Experimental Section); the initial rates are given in Table 1. We found that the initial rates of degradation of Hg−C bonds of MeHgX (0.1 M) by Bme^{Me} (1:1 molar ratio) are ∼2-fold greater than those obtained by Bmm^{OH} or Bmm^{Me} under identical reaction conditions. This observation clearly suggests that the spacer between the two imidazole rings of $[S_2]$-donor ligands (−CH_2− in case of Bmm^{OH} and Bmm^{Me} vs −CH_2CH_2− in case of Bme^{Me}) plays an important role in the cleavage of the Hg−C bond of MeHgX. Interestingly, we have observed that the rates of cleavage of the Hg−C bond of MeHgI induced by $[S_2]$-donor ligands are almost 10-fold faster than those obtained for MeHgCl under identical reaction conditions, indicating that the X group of MeHgX plays an important role in the cleavage of Hg−C bonds of MeHgX induced by $[S_2]$-donor ligands.

X-ray crystal structure analysis and DFT calculations of $[S_2]$-donor ligands showed that the negative charge on the S atoms of Bme^{Me} is comparatively more than the negative charge on the S atoms of Bmm^{OH} or Bmm^{Me} (Table 2). This might be the possible reason for the relatively high reactivity of Bme^{Me} over Bmm^{OH} or Bmm^{Me}. On the other hand, due to the strong interaction between mercury and iodide, the Hg−C bond of MeHgI (2.121 Å) is relatively longer (weaker) than the Hg−C bond of MeHgCl (2.101 Å); hence, the cleavage of the Hg−C bond of MeHgI is expected to occur at a faster rate in comparison to the cleavage of the Hg−C bond of MeHgCl (Table S6 in the Supporting Information). However, unlike the case of MeHgI, the rates of cleavage of the Hg−C bond of ionic $[MeHg]BF_4$ (the Hg−C bond length of $[MeHg]BF_4$ is 2.086 Å) induced by $[S_2]$-donor ligands were found to be extremely

Table 1. Initial Rate of Degradation of $MeHg^+$ Compounds by $[S_2]$-Donor Ligands

	initial rate (M h^{-1})[a]		
ligand	MeHgI	MeHgCl	$[MeHg]BF_4$
Bmm^{Me}	$(1.3 \pm 0.1) \times 10^{-3}$	$(1.75 \pm 0.3) \times 10^{-4}$	$(5.1 \pm 0.3) \times 10^{-5}$
Bmm^{OH}	$(1.26 \pm 0.1) \times 10^{-3}$	$(1.70 \pm 0.1) \times 10^{-4}$	$(4.9 \pm 0.02) \times 10^{-5}$
Bme^{Me}	$(2.76 \pm 0.3) \times 10^{-3}$	$(3.64 \pm 0.5) \times 10^{-4}$	$(7.6 \pm 1.5) \times 10^{-5}$

[a]All experiments were done in an NMR tube at room temperature (21 °C) in DMSO-d_6 ([MeHgX] = 0.1 M).

DOI: 10.1021/acs.inorgchem.7b01048
Inorg. Chem. XXXX, XXX, XXX−XXX

Table 2. C−S Bond Lengths, Bond Orders, and Charge on the S Atoms of [S_2]-Donor Ligands

	C−S bond length (Å)		
ligand	exptl	calcd[a]	charge on S (au)[a]
Bmm^{Me}	1.682[b]	1.448	−0.294
Bmm^{OH}	1.686, 1.684	1.444, 1.437	−0.298, −0.304
Bme^{Me}	1.682[c]	1.434	−0.319

[a]Optimization and NBO analysis were performed at the B3LYP/6-311++G(2d,p) level of theory. [b]Obtained from ref 22a. [c]Obtained from ref 30f.

slow, almost 100-fold slower than the rates of cleavage of the Hg−C bond of MeHgI induced by [S_2]-donor ligands under identical reaction conditions. In fact, we have observed only ∼15−20% cleavage of Hg−C bonds of MeHgCl and [MeHg]BF_4 after 7 days at room temperature (21 °C). However, the amounts of cleaved products increased at higher temperature (37 °C). We do need further study in the future to identify a better molecule which can facilitate the cleavage of the Hg−C bond of [MeHg]BF_4 at a faster rate at room temperature. Unlike the crystal structure of $[(Bmm^{Me})HgI_2]_m \cdot (MeHgI)_n$, where two S atoms of Bmm^{Me} are weakly coordinated to two different Hg(II) atoms (d_{Hg1-S1} = 2.620 Å and $d_{Hg1'-S2}$ = 2.615 Å), leading to the formation of a polymeric structure, the single-crystal X-ray structure of $(Bme^{Me})HgI_2$, (CCDC 1544311) showed that both S atoms of Bme^{Me} are coordinated equally strongly to the same Hg(II) atom (d_{Hg1-S1} = 2.578 Å) (Figure 14).

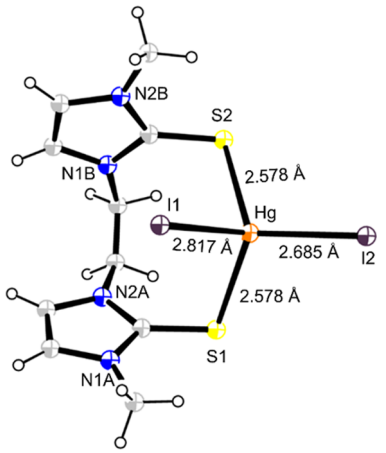

Figure 14. ORTEP diagram of $(Bme^{Me})HgI_2$.

The formation of R_2Hg as one of the degradation products in the reactions of RHg^+ with [S_2]-donor ligands (Bmm^{OH}, Bmm^{Me}, and Bme^{Me}) is quite interesting here. Notably, under aerobic conditions a few soil and aquatic microorganisms have shown the unique ability to metabolize phenylmercuric acetate (PhHgOAc) and one of the major metabolic products, identified in this case, was diphenylmercury (Ph_2Hg).[32] Formation of Ph_2Hg was also observed in the reactions of PhHgOAc with different thiol-containing amino acids and 2,3-dimercaptopropanol ($BALH_3$).[33] On the other hand, several sulfate-reducing bacteria showed mercury tolerance due to their ability to convert $MeHg^+$ to insoluble HgS(s) and Me_2Hg.[34−37] In the culture studies with axenic cultures of *D. desulfuricans* strain LS, Baldi and co-workers observed the degradation of soluble $MeHg^+$ to insoluble black metacinnabar (β-HgS), and volatile Me_2Hg.[37] In addition, the formation of Me_2Hg from $MeHg^+$ in the presence of H_2S,[38] inorganic and organic reduced sulfur surfaces,[39] benzimidazole-based thione[28b] has been reported in the literature. Me_2Hg is known to decompose to gaseous CH_4 and $MeHg^+$ in acidic medium.[37,38] We have also noticed that the Me_2Hg obtained in the reaction was decomposed slowly into CH_4 in acidic medium in the presence of an [S_2]-donor ligand.[40]

In summary, in the reactions of [S_2]-donor ligands with RHgX, in a 1:1 molar ratio, we have observed the formation of R_2Hg and different types of tetracoordinated Hg(II) complexes. The R_2Hg produced in the above reactions further decomposed to RH in acidic medium. The possible explanation for the formation of R_2Hg could be due to the exchange of R groups between two mercury centers in solution in the presence of an electron-donating ligand (Bmm^{Me}, Bmm^{Me}, or Bme^{Me}), as illustrated in Figure 15. The exchange of R groups between two mercury centers in solution has been reported in the literature.[41] To confirm the role of the [S_2]-donor ligand in the exchange of R groups between two Hg−R groups, we have treated $(Bmm^{Me})HgMeCl$ with PhHgCl (in 1:1 molar ratio) in

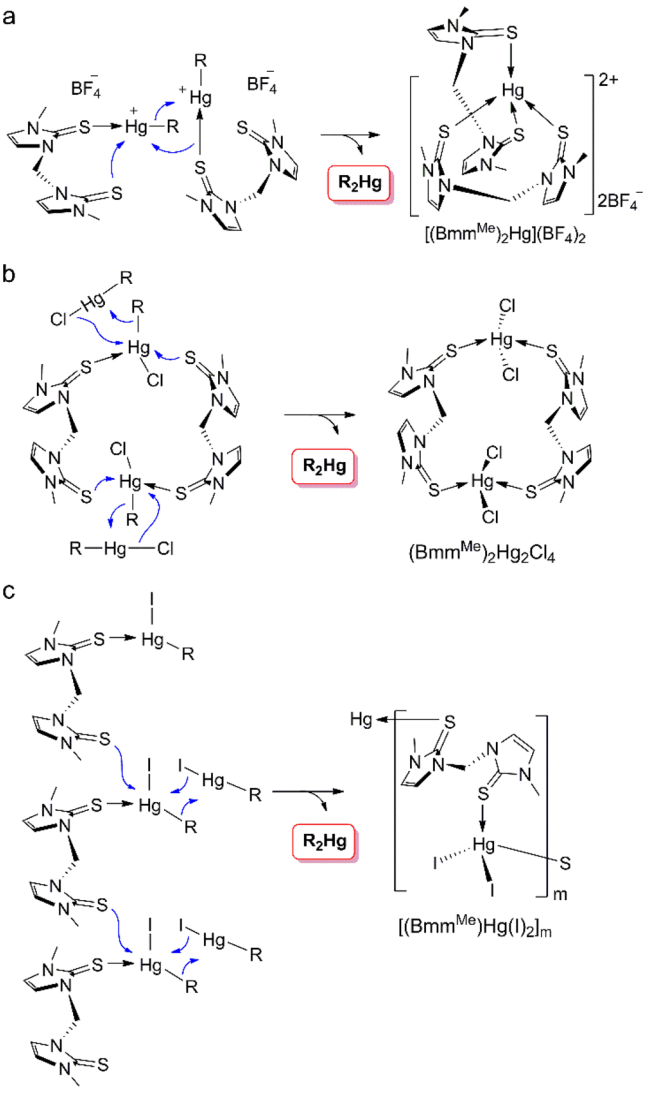

Figure 15. Possible mechanisms for formation of stable tetracoordinated Hg(II) complexes in the reaction of Bmm^{Me} with RHgX, where X = BF_4^- (a), Cl^- (b), I^- (c).

DOI: 10.1021/acs.inorgchem.7b01048
Inorg. Chem. XXXX, XXX, XXX−XXX

methanol/dichloromethane (1/1) solvent at 21 °C, which afforded the unsymmetrical arylalkylmercury compound PhHgMe along with the other expected products Ph_2Hg, Me_2Hg, and $[(Bmm^{Me})_2Hg_2Cl_4]$.

The $^2J(^{199}Hg-^1H)$ coupling constant values for Me_2Hg, PhHgMe, and $(Bmm^{Me})HgMeCl$ in DMSO-d_6 are 105, 113, and 221 Hz respectively (Figure 16).[42] PhHgMe was isolated

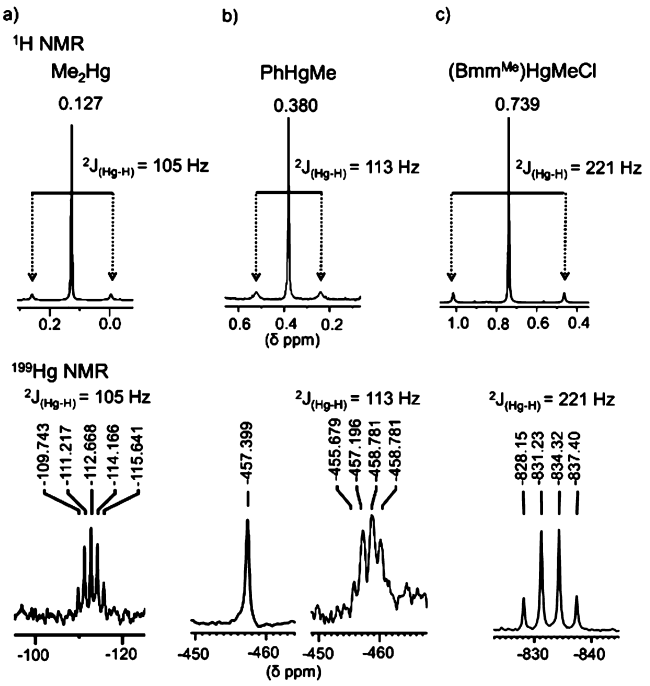

Figure 16. ^{1}H (showing only the signal of the Hg−CH_3 group) and ^{199}Hg NMR spectra of Me_2Hg (a), PhHgMe (b), and (Bmm^{Me})-HgMeCl (c) showing $^2J(^{199}Hg-^1H)$ coupling constants in DMSO-d_6.

from the above reaction mixture by extracting with nonpolar solvent and characterized thoroughly (Figure 16 and Figure S41 in the Supporting Information). However, the treatment of MeHgCl with PhHgCl in a 1:1 molar ratio in the absence of any electron-donating ligand Bmm^{Me} did not produce PhHgMe, Ph_2Hg, and Me_2Hg at room temperature in 2 h (this reaction was performed in an NMR tube in DMSO-d_6). These observations suggest that in the presence of an electron-donating $[S_2]$-donor ligand (in 1:1 molar ratio), the Hg−R bonds in 1:1 RHg-conjugated complexes $[(Bmm^{Me})HgR]X$ (X = BF_4^-) and $(Bmm^{Me})HgRX$ (X = Cl^-, I^-) are activated and, therefore, undergo facile exchange between them (with another molecule of 1:1 RHg-conjugated complex) or with the another molecule of RHgX present in the solution. This possible mechanism is also well supported by the isolation of crystals of free ligand Bmm^{Me} from the reaction mixture of Bmm^{Me} plus MeHgCl (1:1 molar ratio) and the isolation of crystals of $[(Bmm^{Me})HgI_2]_m\cdot(MeHgI)_n$ from the reaction mixture of Bmm^{Me} plus MeHgI (1:1 molar ratio), where MeHgI is cocrystallized with the cleaved product $[(Bmm^{Me})HgI_2]_m$.

In conclusion, we have demonstrated that the $[S_2]$-donor ligands facilitate the cleavage of Hg−C bonds of various organomercurials RHgX (R = Me, Et, Ph; X = BF_4^-, Cl^-, I^-). The reactions of Bmm^{OH}, Bmm^{Me}, and Bme^{Me} with RHgX afforded the formation of tetracoordinated Hg(II) complexes and R_2Hg, which is further degraded to RH in acidic medium. Our experimental results show that the rates of cleavage of the Hg−C bonds of MeHgX induced by $[S_2]$-donor ligands (Bmm^{OH}, Bmm^{Me}, and Bme^{Me}) are highly dependent on the X group present in MeHgX and the spacer between the two imidazole rings of $[S_2]$-donor ligands. The rates of cleavage of the Hg−C bond of MeHgI induced by $[S_2]$-donor ligands are found to be almost 10−100-fold faster than the rates obtained for MeHgCl and $[MeHg]BF_4$, respectively, under identical reaction conditions. Moreover, the rate of degradation of MeHgI by Bme^{Me} is almost 2-fold faster than the rate of degradation of MeHgI by Bmm^{OH} or Bmm^{Me}. Interestingly, we noticed that the nature of the stable tetracoordinated Hg(II) complexes also depends critically on the X group of RHgX and the $[S_2]$-donor ligands used for the cleavage of Hg−C bonds. For example, the reactions of Bmm^{Me} with ionic $[RHg]BF_4$ afforded the formation of the mononuclear mercury complex $[(Bmm^{Me})_2Hg](BF_4)_2$, where both S atoms of Bmm^{Me} are coordinated to the same Hg(II) atom in an unsymmetrical manner and BF_4^- serves as a counteranion. However, the reactions of Bmm^{Me} with RHgCl afforded the formation of $(Bmm^{Me})_2Hg_2Cl_4$, where the two S atoms of Bmm^{Me} are coordinated to the two different Hg(II) atoms, resulting in the formation of a stable 16-membered cyclic dinuclear mercury complex. On the other hand, treatment of Bmm^{Me} with MeHgI afforded a polymeric structure of $[(Bmm^{Me})HgI_2]_m\cdot(MeHgI)_n$, in which MeHgI is cocrystallized with the cleaved product. However, a similar reaction with Bme^{Me} afforded the formation of the discrete mononuclear mercury compound $(Bme^{Me})HgI_2$. A common feature of all three of these structures, $(Bmm^{Me})_2Hg_2Cl_4$, $[(Bmm^{Me})HgI_2]_m\cdot(MeHgI)_n$, and (Bme^{Me})-HgI_2, is that the halides are covalently attached with the mercury center. Our finding may help in understanding the coordination behavior of various organomercurials with $[S_2]$-donor ligands and the mechanism of cleavage of Hg−C bonds of organomercurials by many aquatic microorganisms.

EXPERIMENTAL SECTION

Caution! Organomercurials are highly toxic to humans, and thus appropriate safety precautions must be taken in handling these toxic chemicals.

General Experimental Considerations. Imidazole, phenylmercury chloride, methylmercury iodide, and ethylmercury chloride were purchased from Alfa Aesar. Methylmercury chloride and sulfur powder were purchased from Sigma-Aldrich, and other chemicals were purchased from local companies. All experiments were carried out under anhydrous and anaerobic conditions using standard Schlenk techniques for the synthesis. Electrospray ionization high-resolution mass spectrometry (ESI-HRMS) was carried out with an Agilent 6540 Q-TOF instrument (Agilent Technologies, USA). ^{1}H (400 MHz), ^{13}C (100 MHz), and ^{199}Hg (71.6 MHz) NMR spectra were obtained on a Bruker Advance 400 NMR spectrometer using the solvent as an internal standard for ^{1}H and ^{13}C. Chemical shifts (^{1}H, ^{13}C) are cited with respect to tetramethylsilane (TMS). ^{199}Hg NMR spectra are reported in ppm relative to neat Me_2Hg (δ 0 ppm), and $HgCl_2$ (δ −1501 ppm for 1 M solution in DMSO-d_6) was used as an external standard.[43]

Synthesis of $[(Bmm^{OH})HgMe]BF_4$. To a solution of MeHgCl (50 mg, 0.2 mmol) in 5 mL of dichloromethane at room temperature (21 °C) was added $AgBF_4$ (38.7 mg, 0.2 mmol). The immediate formation of a white precipitate of AgCl was observed in the above reaction mixture. The suspension was stirred for 3 h and filtered into a flask containing Bmm^{OH} (59.7 mg, 0.2 mmol) in 5 mL of methanol. The resulting solution was stirred for 2 h at 21 °C, and solvent was removed by evaporation to obtain a solid crude product. The crude product was further washed with 5 mL of acetonitrile and Et_2O (2 × 5 mL) and dried under vacuum to give a white solid of $[(Bmm^{OH})$-HgMe]BF_4. Yield: 75.5 mg, 63%. ^{1}H NMR (DMSO-d_6): δ 0.71 (s,

DOI: 10.1021/acs.inorgchem.7b01048
Inorg. Chem. XXXX, XXX, XXX−XXX

3H), 3.65−3.69 (q, J = 4.0 Hz, 4H), 3.98−4.01 (t, J = 4.0 Hz, 4H), 4.95 (t, J = 4.0 Hz, 2H), 6.26 (s, 2H), 7.20−7.21 (d, J = 2.8 Hz, 2H), 7.50−7.50 (d, J = 2.8 Hz, 2H). ^{13}C NMR (DMSO-d_6): δ 8.9, 49.9, 56.3, 58.4, 118.1, 119.7, 159.6. ^{199}Hg NMR (DMSO-d_6): δ −712 (0.1 M at 300 K). HR-ESIMS (m/z): calcd for $C_{12}H_{19}N_4O_2S_2Hg$ $[M]^+$ 517.0648, found 517.0644.

Synthesis of [(Bmm^{OH})HgEt]BF$_4$. [(Bmm^{OH})HgEt]BF$_4$ was synthesized following a procedure similar to that for [(Bmm^{OH})-HgMe]BF$_4$ by using EtHgCl (50 mg, 0.19 mmol) in place of MeHgCl, AgBF$_4$ (36.7 mg, 0.19 mmol), and Bmm^{OH} (56.6 mg, 0.19 mmol). Yield: 78.8 mg, 68%. ^{1}H NMR (DMSO-d_6): δ 1.24−1.28 (t, J = 8.0 Hz, 3H), 1.57−1.64 (q, J = 8.0 Hz, 2H), 3.68−3.71 (t, J = 7.6 Hz, 4H), 4.09−4.12 (t, J = 7.6 Hz, 4H), 5.07 (s, 2H), 6.38 (s, 2H), 7.36 (br s, 2H), 7.59−7.59 (d, J = 2.4 Hz, 2H). ^{13}C NMR (DMSO-d_6): δ 14.1, 24.2, 56.9, 58.6, 118.8, 120.5, 157.1. ^{199}Hg NMR (DMSO-d_6): δ −898 (0.1 M at 300 K). HR-ESIMS (m/z): calcd for $C_{13}H_{21}N_4O_2S_2Hg$ $[M]^+$ 531.0804, found 531.0798.

Synthesis of [(Bmm^{OH})HgPh]BF$_4$. [(Bmm^{OH})HgPh]BF$_4$ was synthesized following a procedure similar to that for [(Bmm^{OH})-HgMe]BF$_4$ by using PhHgCl (50 mg, 0.16 mmol) in place of MeHgCl, AgBF$_4$ (31.1 mg, 0.16 mmol), and Bmm^{OH} (47.9 mg, 0.16 mmol). Yield: 80.3 mg, 76%. ^{1}H NMR (DMSO-d_6): δ 3.65 (br s, 4H), 3.99−4.02 (d, J = 8 Hz, 4H), 4.92 (br s, 2H), 6.19 (s, 2H), 7.115−7.119 (d, J = 1.6 Hz, 2H), 7.16−7.35 (m, 3H), 7.41−7.50 (m, 3H). ^{13}C NMR (DMSO-d_6): δ 49.7, 55.8, 58.3, 117.6, 119.0, 127.8, 128.2, 136.8, 151.4, 161.4. ^{199}Hg NMR (DMSO-d_6): δ −1154 (0.1 M at 300 K). HR-ESIMS (m/z): calcd for $C_{17}H_{21}N_4O_2S_2Hg$ $[M]^+$ 579.0805, found 579.0793.

Synthesis of [(Bmm^{OH})$_2$Hg](BF$_4$)$_2$. To obtain the cleaved product [(Bmm^{OH})$_2$Hg](BF$_4$)$_2$, the 1:1 complex [(Bmm^{OH})HgPh]BF$_4$ (100 mg, 0.15 mmol) was stirred in acetonitrile/water (1/1) solution for 48 h at 37 °C. The solvents were evaporated, and the residue was washed several times with the nonpolar solvent hexane (4 × 5 mL) to remove Ph_2Hg followed by Et_2O (2 × 5 mL) to obtain a white solid of [(Bmm^{OH})$_2$Hg](BF$_4$)$_2$.Yield: 52.6 mg, 36%. ^{1}H NMR (DMSO-d_6): δ 3.70−3.71 (t, J = 5.2 Hz, 8H), 4.13−4.17 (t, J = 5.6 Hz, 8H), 4.94−4.96 (t, J = 4.8 Hz, 4H), 6.61 (s, 4H), 7.54−7.55 (d, J = 2.4 Hz, 2H), 7.89−7.90 (d, J = 2.4 Hz, 2H). ^{13}C NMR (DMSO-d_6): δ 50.7, 57.3, 58.5, 120.1, 122.0, 154.0. ^{199}Hg NMR (DMSO-d_6): δ −443 (0.05 M at 300 K). HR-ESIMS (m/z): calcd for $C_{22}H_{32}N_8O_4S_4Hg$ $[M]^{2+}$ 401.0560, found 401.0538.

Synthesis of [(Bmm^{Me})HgMe]BF$_4$. To a solution of MeHgCl (50 mg, 0.2 mmol) in 5 mL of dichloromethane at room temperature (21 °C) was added AgBF$_4$ (38.7 mg, 0.2 mmol). The immediate formation of AgCl precipitate was observed. The suspension was stirred for 3 h and filtered into a solution of Bmm^{Me} (48.1 mg, 0.2 mmol) in 5 mL of dichloromethane. The resulting solution was stirred for 2 h at 21 °C, and solvent was removed by evaporation. The residue was washed with Et_2O (3 × 5 mL), and volatile components were removed under vacuum pressure to afford [(Bmm^{Me})HgMe]BF$_4$ as a white solid. Yield: 65 mg, 60%. ^{1}H NMR (DMSO-d_6): δ 0.74 (s, 3H), 3.56 (s, 6H), 6.41 (s, 2H), 7.46−7.47 (d, J = 4.0 Hz, 2H), 7.68−7.69 (d, J = 4.0 Hz, 2H). ^{13}C NMR (DMSO-d_6): δ 8.5, 35.3, 57.4, 119.7, 121.4, 155.1. ^{199}Hg NMR (DMSO-d_6): δ −750 (0.1 M at 300 K). HR-ESIMS (m/z): calcd for $C_{10}H_{15}N_4S_2Hg$ $[M]^+$ 457.0436, found 457.0467.

Synthesis of [(Bmm^{Me})HgEt]BF$_4$. [(Bmm^{Me})HgEt]BF$_4$ was synthesized following a procedure similar to that for [(Bmm^{Me})-HgMe]BF$_4$ by using EtHgCl (50 mg, 0.19 mmol) in place of MeHgCl, AgBF$_4$ (36.7 mg, 0.19 mmol), and Bmm^{Me} (45.6 mg, 0.19 mmol). Yield: 60 mg, 68%. ^{1}H NMR (DMSO-d_6): δ 1.22−1.26 (t, J = 7.6 Hz, 2H), 1.60−1.64 (q, J = 7.6 Hz, 2H), 3.47 (s, 6H), 6.16 (s, 2H), 7.12−7.13 (d, J = 1.6 Hz, 2H), 7.41−7.410 (d, J = 1.6 Hz, 2H). ^{13}C NMR (DMSO-d_6): δ 13.8, 22.6, 34.5, 56.1, 117.7, 118.9, 162.0. ^{199}Hg NMR (DMSO-d_6): δ −873 (0.1 M at 300 K). HR-ESIMS (m/z): calcd for $C_{11}H_{17}N_4S_2Hg$ $[M]^+$ 471.0592, found 471.0633.

Synthesis of [(Bmm^{Me})HgPh]BF$_4$. [(Bmm^{Me})HgPh]BF$_4$ was synthesized following a procedure similar to that for [(Bmm^{Me})-HgMe]BF$_4$ by using PhHgCl (50 mg, 0.16 mmol) instead of MeHgCl, AgBF$_4$ (31.1 mg, 0.16 mmol), and Bmm^{Me} (38.4 mg, 0.16 mmol). Yield: 71.6 mg, 74%. ^{1}H NMR (DMSO-d_6): δ 3.48 (s, 6H), 6.18 (s, 2H), 7.15 (br s, 2H), 7.20−7.41 (m, 5H), 7.43 (br s, 2H). ^{13}C NMR (DMSO-d_6): δ 34.6, 56.1, 117.8, 119.0, 127.8, 128.2, 136.7, 151.6, 161.5. ^{199}Hg NMR (DMSO-d_6): δ −1154 (0.1 M at 300 K). HR-ESIMS (m/z): calcd for $C_{15}H_{17}N_4S_2Hg$ $[M]^+$ 519.0593, found 519.0627.

Synthesis of [(Bmm^{Me})$_2$Hg](BF$_4$)$_2$. To obtain the cleaved product [(Bmm^{Me})$_2$Hg](BF$_4$)$_2$, the 1:1 complex [(Bmm^{Me})HgPh]BF$_4$ (100 mg, 0.16 mmol) was stirred in acetonitrile/water (1/1) solution for 48 h at 37 °C. Then the solvents were removed under vacuum and the residue was washed several times with the nonpolar solvent hexane (4 × 5 mL) to remove Ph_2Hg followed by Et_2O (2 × 5 mL) to obtain [(Bmm^{me})$_2$Hg](BF$_4$)$_2$ as a white solid. Yield: 62.1 mg, 44%. A suitable single crystal was obtained by slow evaporation of an ACN/DMSO (2/1) solution.^{1}H NMR (DMSO-d_6): δ 3.58 (s, 12H), 6.49 (s, 4H), 7.52 (br s, 4H), 7.58 (br s, 4H). ^{13}C NMR (DMSO-d_6): δ 35.6, 57.0, 119.3, 121.8, 154.8. ^{199}Hg NMR (DMSO-d_6): δ −719 (0.05 M at 300 K). HR-ESIMS (m/z): calcd for $C_{18}H_{24}N_8S_4Hg$ $[M]^{2+}$ 341.0348, found 341.0377.

Synthesis of (Bmm^{Me})HgMeCl. To a solution of Bmm^{Me} (50 mg, 0.21 mmol) in 10 mL of dichloromethane was added MeHgCl (52.2 mg, 0.21 mmol), and the resulting suspension was stirred for 2 h at 21 °C. The volatile components were removed by evaporation, and the residue was washed with Et_2O (2 × 5 mL) and then dried over high vacuum pressure to give (Bmm^{Me})HgMeCl as a white powder. Yield: 70.1 mg, 68%. ^{1}H NMR (DMSO-d_6): δ 0.74 (s, 1H), 3.47 (s, 6H), 6.15 (s, 2H), 7.13−7.13 (d, J = 4.0 Hz, 2H), 7.41−7.42 (d, J = 4.0 2H). ^{13}C NMR (DMSO-d_6): δ 5.9, 34.5, 56.0, 117.7, 118.9, 162.2. ^{199}Hg NMR (DMSO-d_6): δ −837 (0.1 M at 300 K). HR-ESIMS (m/z): calcd for $C_{10}H_{15}N_4S_2HgCl$ $[M]^+$ 492.0115, found $C_{10}H_{15}N_4S_2Hg$ $[M - Cl]^+$ 457.0467.

Synthesis of (Bmm^{Me})HgEtCl. (Bmm^{Me})HgEtCl was synthesized following a procedure similar to that for (Bmm^{Me})HgMeCl, except EtHgCl (55.1 mg, 0.21 mmol) was added in place of MeHgCl. Yield: 75.3 mg, 71%. ^{1}H NMR (DMSO-d_6): δ 1.23−1.27 (t, J = 7.8 Hz, 3H), 1.61−1.67 (q, J = 7.8 Hz, 2H), 3.46 (s, 6H), 6.14 (s, 2H), 7.13−7.13 (d, J = 2.4 Hz, 2H), 7.40−7.41 (d, J = 2.4 Hz, 2H). ^{13}C NMR (DMSO-d_6): δ 13.7, 22.4, 34.5, 56.0, 117.6, 118.8, 162.34. ^{199}Hg NMR (DMSO-d_6): δ −993 (0.1 M at 300 K). HR-ESIMS (m/z): calcd for $C_{11}H_{17}N_4S_2HgCl$ $[M]^+$ 506.0271, found $C_{11}H_{17}N_4S_2Hg$ $[M - Cl]^+$ 471.0633.

Synthesis of (Bmm^{Me})HgPhCl. (Bmm^{Me})HgPhCl was synthesized following a procedure similar to that for (Bmm^{Me})HgMeCl, except PhHgCl (65.1 mg, 0.21 mmol) was added in place of MeHgCl. Yield: 91.8 mg, 79%.^{1}H NMR (DMSO-d_6): δ 3.48 (s, 6H), 6.18 (s, 2H), 7.15−7.16 (d, J = 4.0 Hz, 2H), 7.20−7.35 (m, 3H), 7.42−7.45 (m, 3H). ^{13}C NMR (DMSO-d_6): δ 34.5, 56.1, 117.7, 118.9, 127.8, 128.2, 136.7, 151.3, 161.9. ^{199}Hg NMR (DMSO-d_6): δ −1160 (0.1 M at 300 K). HR-ESIMS (m/z): calcd for $C_{15}H_{17}N_4S_2HgCl$ $[M]^+$ 554.0272, found $C_{15}H_{17}N_4S_2Hg$ $[M - Cl]^+$ 519.0627.

Synthesis of (Bmm^{Me})$_2$Hg$_2$Cl$_4$. (Bmm^{Me})$_2$Hg$_2$Cl$_4$ was obtained from the reaction solution of (Bmm^{Me})HgPhCl (100 mg, 0.18 mmol) in acetonitrile/water (1/1) after stirring for 48 h at 37 °C. Solvent was removed under reduced pressure, and the resulting precipitate was washed several times with hexane (2 × 5 mL) to remove Ph_2Hg followed by Et_2O (2 × 5 mL) to obtain the cleaved product (Bmm^{Me})$_2$Hg$_2$Cl$_4$ as a white solid. Yield: 72.4 mg, 42%. The pure compound (Bmm^{Me})$_2$Hg$_2$Cl$_4$ was crystallized in various solvents to obtain suitable single crystals of (Bmm^{Me})$_2$Hg$_2$Cl$_4$, which was always cocrystallized with the solvent molecules, as confirmed by an X-ray structure determination. ^{1}H NMR (DMSO-d_6): δ 3.62 (s, 12H), 6.57 (s, 2H), 7.53−7.54 (d, J = 4.0 Hz, 2H), 7.85−7.85 (d, J = 4.0 Hz, 2H). ^{13}C NMR (DMSO-d_6): δ 35.8, 57.3, 120.3, 122.1, 154.1. ^{199}Hg NMR (DMSO-d_6): δ −886 (0.05 M at 300 K). HR-ESIMS (m/z): calcd for $C_{18}H_{24}N_8S_4Hg_2Cl_4$ $[M + H]^+$ 1023.95, found $[M - HgCl_3]^+$ 717.0430, $[M - C_9H_{12}N_4S_2HgCl_3]^+$ 476.9911.

Synthesis of (Bmm^{OH})HgMeCl. To a solution of Bmm^{OH} (50 mg, 0.16 mmol) in 10 mL of methanol was added MeHgCl (52.2 mg, 0.16 mmol), and the resulting suspension was stirred for 2 h at 21 °C. The volatile components were removed by evaporation, and the residue was washed with Et_2O (2 × 5 mL) and then dried over high vacuum

DOI: 10.1021/acs.inorgchem.7b01048
Inorg. Chem. XXXX, XXX, XXX−XXX

pressure to give (Bmm^{OH})HgMeCl as a white solid. Yield: 54.7 mg, 62%. ^{1}H NMR (DMSO-d_6): δ 0.74 (s, 3H), 3.63−3.67 (q, J = 4.0 Hz, 4H), 3.99−4.01 (t, J = 4.0 Hz, 4H), 4.90−4.92 (t, J = 4.0 Hz, 2H), 6.18 (s, 2H), 7.09−7.10 (d, J = 2.8 Hz, 2H), 7.43−7.43 (d, J = 2.8 Hz, 2H). ^{13}C NMR (DMSO-d_6): δ 5.85, 49.6, 55.7, 58.2, 117.5, 118.9, 162.0. ^{199}Hg NMR (DMSO-d_6): −842 (0.1 M at 300 K). HR-ESIMS (m/z): calcd for $C_{12}H_{19}N_4O_2S_2HgCl$ $[M]^+$ 552.0326, found $C_{12}H_{19}N_4O_2S_2Hg$ $[M - Cl]^+$ 517.0644.

Synthesis of (Bmm^{OH})HgEtCl. (Bmm^{OH})HgEtCl was synthesized following a procedure similar to that for (Bmm^{OH})HgMeCl, except EtHgCl (42.4 mg, 0.16 mmol) was added in place of MeHgCl. Yield: 59.7 mg, 66%. ^{1}H NMR (DMSO-d_6): δ 1.23−1.25 (t, J = 8.0 Hz, 3H), 1.61−1.67 (q, J = 8.0 Hz, 2H), 3.63−3.71 (q, J = 5.2 Hz, 4H), 3.98−4.01 (t, J = 5.2 Hz, 4H), 4.91−4.93 (t, J = 5.20 Hz, 2H), 6.18 (s, 2H), 7.09−7.10 (d, J = 2.4 Hz, 2H), 7.43−7.43 (d, J = 2.4 Hz, 2H). ^{13}C NMR (DMSO-d_6): δ 13.8, 22.6, 49.6, 55.7, 58.2, 117.5, 118.9, 162.0. ^{199}Hg NMR (DMSO-d_6): δ −1004 (0.1 M at 300 K). HR-ESIMS (m/z): calcd for $C_{13}H_{21}N_4O_2S_2HgCl$ $[M]^+$ 566.0483, found $C_{13}H_{21}N_4O_2S_2Hg$ $[M - Cl]^+$ 531.0798.

Synthesis of (Bmm^{OH})HgPhCl. (Bmm^{OH})HgPhCl was synthesized following a procedure similar to that for (Bmm^{Me})HgMeCl, except PhHgCl (52.1 mg, 0.16 mmol) was added in place of MeHgCl. Yield: 70.6 mg, 72%. ^{1}H NMR (DMSO-d_6): δ 3.64−3.67 (t, J = 5.2 Hz, 4H), 3.99−4.01 (t, J = 5.2 Hz, 4H), 4.93 (br s, 2H), 6.20 (s, 2H), 7.11−7.12 (d, J = 1.6 Hz, 2H), 7.19−7.22 (t, J = 7.2 Hz, 1H), 7.26−7.30 (t, J = 7.2 Hz, 2H), 7.41−7.43 (d, J = 7.2 Hz, 2H), 7.45−7.46 (t, J = 1.6 Hz, 2H). ^{13}C NMR (DMSO-d_6): δ 49.7, 55.8, 58.3, 117.7, 119.1, 127.8, 128.2, 136.8, 151.9, 161.4. ^{199}Hg NMR (DMSO-d_6): δ −1156 (0.1 M at 300 K). HR-ESIMS (m/z): calcd for $C_{17}H_{21}N_4O_2S_2HgCl$ $[M]^+$ 614.0484, found $C_{17}H_{21}N_4O_2S_2Hg$ $[M - Cl]^+$ 579.0793.

Synthesis of [(Bmm^{OH})$_2$$Hg_2Cl_4$]. ($Bmm^{OH}$)$_2$$Hg_2Cl_4$ was synthesized following a procedure similar to that for (Bmm^{Me})$_2$$Hg_2Cl_4$, except ($Bmm^{OH}$)HgPhCl (100 mg, 0.16 mmol) was added in place of (Bmm^{Me})HgPhCl. Yield: 100 mg, 54%. ^{1}H NMR (DMSO-d_6): δ 3.69−3.72 (t, J = 5.4 Hz, 8H), 4.13−4.17 (br s, 8H), 4.97 (s, 4H), 6.61 (s, 4H), 7.56 (br s, 4H), 7.90−7.91 (d, J = 2.4 Hz, 4H), ^{13}C NMR (DMSO-d_6): δ 51.0, 57.2, 58.5, 120.6, 122.2, 152.3. HR-ESIMS (m/z): calcd for $C_{22}H_{32}N_8S_4O_4Hg_2Cl_4$ $[M + H]^+$: 1143.9541, found $[M - HgCl_3]^+$ 837.0792, $[M - C_{11}H_{16}N_4S_2O_2HgCl_3]^+$ 537.0085.

Synthesis of (Bmm^{Me})HgMeI. To a solution of Bmm^{Me} (50 mg, 0.21 mmol) in 10 mL of dichloromethane was added MeHgI (71.2 mg, 0.21 mmol), and the reaction mixture was stirred for 2 h at 21 °C. The solvent was removed by evaporation, the residue was washed with Et_2O (2 × 5 mL), and volatile components were removed under vacuum pressure to give (Bmm^{Me})HgMeI as a white solid. Yield: 70.3 mg, 58%. ^{1}H NMR (DMSO-d_6): δ 0.89 (s, 1H), 3.47 (s, 6H), 6.14 (s, 2H), 7.13−7.13 (d, J = 2.4 Hz, 2H), 7.40−7.41 (d, J = 2.4 Hz, 2H). ^{13}C NMR (DMSO-d_6): δ 14.7, 35.0, 56.5, 118.2, 119.3, 162.9. ^{199}Hg NMR (DMSO-d_6): δ −1133 (0.1 M at 300 K). HR-ESIMS (m/z): calcd for $C_{10}H_{15}N_4S_2HgI$ $[M]^+$ 583.9481, found $C_{10}H_{15}N_4S_2Hg$ $[M - I]^+$ 457.0467.

Synthesis of [(Bmm^{Me})HgI_2]$_m$·($MeHgI$)$_n$. To obtain the cleavage product [(Bmm^{Me})HgI_2]$_m$·($MeHgI$)$_n$, we stirred the 1:1 complex (Bmm^{Me})HgMeI (25 mg, 0.043 mmol) in 5 mL of methanol for 48 h at 37 °C. The solvent was removed, and the crude product was washed several times with acetonitrile followed by Et_2O (2 × 5 mL). The product was dried under reduced pressure for several hours to obtain a yellow solid of [(Bmm^{Me})HgI_2]$_m$·($MeHgI$)$_n$. Yield: 12 mg, 42%. Suitable needle-shaped single crystals were obtained from a methanol solution of [(Bmm^{Me})HgI_2]$_m$·($MeHgI$)$_n$. ^{1}H NMR (DMSO-d_6): δ 3.55 (s, 6H), 6.54 (s, 2H), 7.47−7.48 (d, J = 4.0 Hz, 2H), 7.91−7.92 (d, J = 4.0 Hz, 2H). ^{13}C NMR (DMSO-d_6): δ 35.8, 56.9, 119.8, 121.5, 156.7. ^{199}Hg NMR (DMSO-d_6): δ −2126 (0.025 M at 300 K).

Synthesis of (Bme^{Me})HgMeI. (Bme^{Me})HgMeI was synthesized following a procedure similar to that for (Bmm^{Me})HgMeI, except that Bme^{Me} (53.4 mg, 0.21 mmol) was added in place of Bmm^{Me}. Yield: 95.2 mg, 76%. ^{1}H NMR (DMSO-d_6): δ 0.87 (s, 1H), 3.46 (s, 6H), 4.32 (s, 4H), 6.87−6.88 (d, J = 2.4 Hz, 2H), 7.10−7.11 (d, J = 2.4 Hz, 2H). ^{13}C NMR (DMSO-d_6): δ 14.0, 34.5, 45.2, 117.4, 118.6, 161.0. ^{199}Hg NMR (DMSO-d_6): δ −1092 (0.1 M at 300 K). HR-ESIMS (m/z): calcd for $C_{11}H_{17}N_4S_2HgI$ $[M]^+$ 597.9637, found $C_{11}H_{17}N_4S_2Hg$ $[M - I]^+$ 471.0641.

Synthesis of (Bme^{Me})HgI_2. (Bme^{Me})HgI_2 was synthesized following a procedure similar to that for [(Bmm^{Me})HgI_2]$_m$·($MeHgI$)$_n$, except that (Bme^{Me})HgMeI (25 mg, 0.041 mmol) was added in place of (Bmm^{Me})HgMeI. Yield: 20.1 mg, 69%. Suitable block-type single crystals were obtained by slow evaporation of a methanolic solution of (Bme^{Me})HgI_2. ^{1}H NMR (DMSO-d_6): δ 3.59 (s, 6H), 4.81 (s, 2H), 7.41−7.41 (d, J = 2.0 Hz, 2H), 7.49−7.50 (d, J = 2.0 Hz, 2H). ^{13}C NMR (DMSO-d_6): δ 35.9, 45.5, 120.5, 121.5, 153.6. ^{199}Hg NMR: not observed.

Isolation of Ph_2Hg. The nonpolar product of Ph_2Hg was extracted from the reaction solution of Bmm^{OH} (or Bmm^{Me} or Bme^{Me}) with PhHgCl (1:1 molar ratio) by using hexane. The hexane solution was concentrated and dried under high vacuum to yield a white solid of Ph_2Hg. Yield: ∼22%. ^{1}H NMR (DMSO-d_6): δ 7.13−7.17 (t, J = 7.4 Hz, 2H), 7.32−7.36 (t, J = 7.6 Hz, 4H), 7.51−7.53 (dd, J = 7.8 Hz, 4H). ^{13}C NMR (DMSO-d_6): δ 127.1, 127.8, 138.1, 170.9. ^{199}Hg NMR (DMSO-d_6): δ −814 (0.1 M at 300 K).

Isolation of PhHgMe. To a solution of (Bmm^{OH})HgMeCl or (Bmm^{Me})HgMeCl in chloroform/methanol (1:1) was added 1 equiv of PhHgCl, and the reaction mixture was stirred for 24 h at room temperature. After 24 h, the reaction mixture was extracted by the nonpolar solvent hexane. The solvent was concentrated and dried under high vacuum to yield a white solid of PhHgMe. Yield: ∼14%. ^{1}H NMR (DMSO-d_6): δ 0.36 (s, 3H), 7.09−7.13 (t, J = 7.4 Hz, 2H), 7.29−7.33 (t, J = 7.6 Hz, 4H), 7.41−7.43 (dd, J = 7.8 Hz, 4H). ^{13}C NMR (DMSO-d_6): δ 13.7, 126.8, 127.9, 137.3, 178.1. ^{199}Hg NMR (DMSO-d_6): δ −457 (0.05 M at 300 K).

Synthesis of (Bmm^{OH})$Hg_2Ph_2Cl_2$. To a solution of Bmm^{OH} (25 mg, 0.043 mmol) in 5 mL of methanol was added PhHgCl (27 mg, 0.086 mmol), and the reaction mixture was stirred for 4 h at 21 °C. After completion of the reaction, methanol was removed under vacuum to obtain (Bmm^{OH})$Hg_2Ph_2Cl_2$ as a white precipitate. Suitable single crystals of (Bmm^{OH})$Hg_2Ph_2Cl_2$ were obtained after slow evaporation of the solvent mixture ACN/DMSO (2/1). ^{1}H NMR (DMSO-d_6): δ 3.5 (br s, J = 5.2 Hz, 4H), 3.99−4.01 (t, J = 5.2 Hz, 4H), 4.93 (br s, 2H), 6.20 (s, 2H), 7.11−7.12 (d, J = 1.6 Hz, 2H), 7.19−7.22 (t, J = 7.2 Hz, 1H), 7.26−7.30 (t, J = 7.2 Hz, 2H), 7.41−7.43 (d, J = 7.2 Hz, 2H), 7.45−7.46 (t, J = 1.6 Hz, 2H). ^{13}C NMR (DMSO-d_6): δ 49.7, 55.9, 58.3, 117.7, 119.2, 127.9, 128.2, 136.8, 151.4, 161.2. ^{199}Hg NMR (DMSO-d_6): δ −1177 (0.1 M at 300 K).

Procedure for Kinetic Studies. The cleavage of Hg−C bonds of MeHgX (X = BF_4^-, Cl^-, I^-) induced by [S_2]-donor ligands was followed by ^{1}H NMR spectroscopy, and all experiments were performed in NMR tubes at 21 °C. In general, to a solution of MeHgX (0.1 M) in DMSO-d_6 was added the [S_2]-donor ligand (Bmm^{Me}/Bme^{Me}/Bmm^{OH}) in a 1:1 molar ratio in an NMR tube, and this mixture was kept in a shaker for continuous gentle shaking at 21 °C. ^{1}H NMR spectra were recorded at various times. In order to calculate the rate of demethylation of MeHgX by [S_2]-donor ligands, we used mesitylene (12 mM) as an external standard. Integral values of the singlet resonance of methyl protons ($-CH_3$) of MeHgX (at various time points) with respect to the aromatic singlet resonance of mesitylene (which is considered as 1 and it does not interfere with other signals) were used for calculating the rate. The initial value at 0 min was considered as 100% of MeHgX (0.1 M).

X-ray Crystal Analysis. Crystal structures of these compounds were determined by measuring X-ray diffraction data on a D8 Venture Bruker AXS single-crystal X-ray diffractometer equipped with a CMOS PHOTON 100 detector having monochromatised microfocus sources (Mo Kα = 0.71073 Å). Single crystals of [(Bmm^{Me})$_2$Hg](BF$_4$)$_2$ (CCDC 1534008), [(Bmm^{Me})$_2$$Hg_2Cl_4$]·ACN (CCDC 1534011), [($Bmm^{Me}$)$_2$$Hg_2Cl_4$]·DMF (CCDC 1534012), ($Bmm^{OH}$)$Hg_2Ph_2Cl_2$ (CCDC 1534015), [(Bmm^{Me})HgI_2]$_m$·($MeHgI$)$_n$ (CCDC 1534014), and $Bme^{Me}HgI_2$ (CCDC 1544311) suitable for X-ray diffraction studies were obtained from a slow evaporation process using various solvents.[43] All crystal data were collected at room temperature. Structures were solved using the SHELX program implemented in

DOI: 10.1021/acs.inorgchem.7b01048
Inorg. Chem. XXXX, XXX, XXX−XXX

Table 3. Crystallographic Data and Refinement Parameters for $[(Bmm^{Me})_2Hg](BF_4)_2$ (I), $[(Bmm^{Me})_2Hg_2Cl_4]\cdot 2ACN$ (II), $[(Bmm^{Me})_2Hg_2Cl_4]\cdot 2DMF$ (III), $(Bmm^{OH})Hg_2Ph_2Cl_2$ (IV), $[(Bmm^{Me})HgI_2]_m\cdot(MeHgI)_n$ (V), and $(Bme^{Me})HgI_2$ (VI)

	I	II	III	IV	V	VI
CCDC no.	1534008	1534011	1534012	1534015	1534014	1544311
lattice	triclinic	monoclinic	monoclinic	monoclinic	monoclinic	monoclinic
formula	$C_{18}H_{24}B_2F_8HgN_8S_4$	$C_{22}H_{30}Cl_4Hg_2N_{10}S_4$	$C_{24}H_{38}Cl_4Hg_2N_{10}O_2S_4$	$C_{23}H_{26}Cl_2Hg_2N_4O_2S_2$	$C_{10}H_{15}Hg_2I_3N_4S_2$	$C_{10}H_{12.21}HgI_2N_4S_2$
formula wt	854.9	1105.78	1169.86	926.68	1037.26	706.96
space group	$P\bar{1}$	$C2/m$	$C2/c$	$C2/c$	$P2_1/c$	$Pnma$
a/Å	11.1499(18)	17.3949(14))	18.3396(12)	18.3515(9)	12.1256(12)	9.1474(7)
b/Å	11.791(2)	12.0892(14)	12.3326(12)	14.7223(7)	8.3332(8)	12.9853(9)
c/Å	13.963(2)	10.6711(10)	18.0958(13)	13.7269(6)	21.188(2)	14.4597(10)
α/deg	66.115(7)	90	90	90	90	90
β/deg	68.598(7)	126.202(4)	109.396	111.942(2)	97.800(4)	90
γ/deg	64.060(6)	90	90	90	90	90
V/Å^3	1469.5(4)	1810.8(3)	3860.5(5)	3440.0(3)	2121.1(4)	1717.5(2)
Z	2	2	4	4	4	4
temp/K	300(2)	297(2)	297(2)	298(2)	301(2)	299(2)
radiation (λ)/Å	0.71073	0.71073	0.71073	0.71073	0.71073	0.71073
ρ/g cm^{-3}	1.932	2.028	2.013	1.789	3.248	2.741
μ(Mo Kα)/mm^{-1}	5.598	9.024	8.476	9.214	19.02	12.791
θ_{max}/deg	26.022	25.679	26.024	25.684	26.462	25.682
no. of data collected	25314	31550	69460	32252	53466	16589
no. of data	5790	1809	3803	3287	4263	1694
no. of params	388	108	213	150	194	93
R1 ($I > 2\sigma(I)$)	0.041	0.018	0.018	0.0457	0.034	0.0258
wR2 ($I > 2\sigma(I)$)	0.099	0.042	0.037	0.1347	0.075	0.0615
R1 (all data)	0.052	0.02	0.024	0.0544	0.062	0.0277
wR2 (all data)	0.105	0.042	0.039	0.1418	0.0862	0.0625
R_{int} (all data)	0.0568	0.0557	0.0458	0.0831	0.0952	0.0428
GOF	1.017	1.037	1.035	1.064	1.026	1.136

APEX3.[43−48] The non-H atoms were located in successive difference Fourier syntheses and refined with anisotropic thermal parameters. All hydrogen atoms were placed at calculated positions and refined using a riding model with appropriate HFIX commands. The program Mercury was used for molecular packing analysis.[49] The disordered fluorine atoms (F1, F2, F3, F5, F7, and F8) of $[(Bmm^{Me})_2Hg](BF_4)_2$ were treated using the PART command with occupancy 36%:64% (FA:FB). In addition, the anisotropic displacement parameters for disordered fluorine atoms were fixed using the EADP restraint.[50] The crystal structure of $(Bmm^{OH})Hg_2Ph_2Cl_2$ has disorder in the solvent molecules, which was removed by the SQUEEZE option using PLATON software.[51] Crystallographic data and refinement parameters for **I**−**VI** are given in Table 3.

Computational Details. All the calculations were carried out using B3LYP level of theory as implemented in the Gaussian 09 package.[52] The 6-311++G(2d,p) basis set was used for all atoms (except Hg and I), whereas the Stuttgart−Dresden basis set (SDD) was used for Hg and I atoms with respective relativistic effective core potentials.[53] Frequency calculations of all the optimized structures were performed to ensure that the optimized structures were the local energy minima structure without any imaginary frequencies. The NBO Version 3.1 program implemented in Gaussian 03 was used to perform NPA.[54]

■ ASSOCIATED CONTENT

Supporting Information

The Supporting Information is available free of charge on the ACS Publications website at DOI: 10.1021/acs.inorgchem.7b01048.

Synthesis methods, HR-ESIMS analysis of compounds, ^{1}H, ^{13}C, and ^{199}Hg NMR spectra of [S_2-donor ligands and their complexes with RHgX, DFT calculations, and optimized geometries and coordinates of the optimized structures (PDF)

Accession Codes

CCDC 1517829, 1534008, 1534011−1534012, 1534014−1534015, and 1544311 contain the supplementary crystallographic data for this paper. These data can be obtained free of charge via www.ccdc.cam.ac.uk/data_request/cif, or by emailing data_request@ccdc.cam.ac.uk, or by contacting The Cambridge Crystallographic Data Centre, 12 Union Road, Cambridge CB2 1EZ, UK; fax: +44 1223 336033.

■ AUTHOR INFORMATION

Corresponding Author

*E-mail for G.R.: Gouriprasanna.Roy@snu.edu.in.

ORCID

Gouriprasanna Roy: 0000-0002-0047-3575

Author Contributions

G.R. and R.K. planned the research work, designed experiments, and wrote the manuscript. R.K. carried out most of the experiments mentioned in this paper. R.K., M.B., K.K.J., and A.C. solved the crystal structures. G.R. and R.K. analyzed and interpreted data.

Notes

The authors declare no competing financial interest.

■ ACKNOWLEDGMENTS

We are grateful to Prof. Rupamanjari Ghosh (VC, SNU) for continuous support and encouragement. R.K., M.B., K.K.J., and A.C. thank the SNU for fellowships. We thank the SNU and SERB (SB/S1/IC-44/2013), government of India, for financial support.

DOI: 10.1021/acs.inorgchem.7b01048
Inorg. Chem. XXXX, XXX, XXX−XXX

REFERENCES

(1) (a) Clarkson, T. W.; Magos, L. The Toxicology of Mercury and Its Chemical Compounds. *Crit. Rev. Toxicol.* **2006**, *36*, 609−662. (b) Mutter, J.; Naumann, J.; Guethlin, C. Comments on the Article "The Toxicology of Mercury and Its Chemical Compounds" by Clarkson and Magos (2006). *Crit. Rev. Toxicol.* **2007**, *37*, 537−549. (c) Clarkson, T. W. The toxicology of mercury. *Crit. Rev. Clin. Lab. Sci.* **1997**, *34*, 369−403. (d) Myers, G. J.; Davidson, P. W. Prenatal methylmercury exposure and children: neurologic, developmental, and behavioral research. *Environ. Health Perspect.* **1998**, *106*, 841−847. (e) Magos, L.; Clarkson, T. W. Overview of the clinical toxicity of mercury. *Ann. Clin. Biochem.* **2006**, *43*, 257−268. (f) Berlin, M.; Zalups, R. K.; Fowler, B. A. *Mercury. Handbook on the Toxicology of Metals*, 3rd ed.; Elsevier Academic: San Diego, CA, 2007; Chapter 33, pp 675−729.

(2) (a) Farina, M.; Rocha, J. B. T.; Aschner, M. Mechanisms of methylmercury-induced neurotoxicity: evidence from experimental studies. *Life Sci.* **2011**, *89*, 555−563. (b) Guzzi, G.; La Porta, C. A. M. Molecular mechanisms triggered by mercury. *Toxicology* **2008**, *244*, 1−12. (c) Ballatori, N.; Clarkson, T. W. Biliary secretion of glutathione and of glutathione-metal complexes. *Fundam. Appl. Toxicol.* **1985**, *5*, 816−831. (d) Clarkson, T. W. The three modern faces of mercury. *Environ. Health Perspect.* **2002**, *110*, 11−23.

(3) Wang, F.; Lemes, M.; Khan, M. A. K. In *Environmental Chemistry and Toxicology of Mercury*; Cai, Y., Liu, G., O'Driscoll, N., Eds.; Wiley: Hoboken, NJ, 2012; Chapter 16.

(4) (a) Yin, Z.; Jiang, H.; Syversen, T.; Rocha, J. B. T.; Farina, M. The methylmercury-l-cysteine conjugate is a substrate for the L-type large neutral amino acid transporter. *J. Neurochem.* **2008**, *107*, 1083−1090. (b) Aschner, M.; Aschner, J. L. Mercury neurotoxicity: mechanisms of blood-brain barrier transport. *Neurosci. Biobehav. Rev.* **1990**, *14*, 169−176. (c) Carvalho, C. M. L.; Chew, E.-H.; Hashemy, S. I.; Lu, J.; Holmgren, A. Inhibition of the human thioredoxin system a molecular mechanism of mercury toxicity. *J. Biol. Chem.* **2008**, *283*, 11913−11923.

(5) Khan, M. A.; Wang, F. Mercury-selenium compounds and their toxicological significance: Toward a molecular understanding of the mercury-selenium antagonism. *Environ. Toxicol. Chem.* **2009**, *28*, 1567−1577.

(6) (a) Simmons-Willis, T. A.; Koh, A. S.; Clarkson, T. W.; Ballatori, N. Transport of a neurotoxicant by molecular mimicry: the methylmercury−l-cysteine complex is a substrate for human L-type large neutral amino acid transporter (LAT) 1 and LAT2. *Biochem. J.* **2002**, *367*, 239−246.

(7) (a) Korbas, M.; Krone, P. H.; Pickering, I. J.; George, G. N. Dynamic accumulation and redistribution of methylmercury in the lens of developing zebrafish embryos and larvae. *J. Biol. Inorg. Chem.* **2010**, *15*, 1137−1145. (b) Hoffmeyer, R. E.; Singh, S. P.; Doonan, C. J.; Roos, A. R. S.; Hughes, R. J.; Pickering, I. J.; George, G. N. Molecular mimicry in mercury toxicology. *Chem. Res. Toxicol.* **2006**, *19*, 753−759.

(8) (a) Harris, H. H.; Pickering, I. J.; George, G. N. The chemical form of mercury in fish. *Science* **2003**, *301*, 1203. (b) Stern, A. H.; Hudson, R. J. M.; Shade, C. W.; Ekino, S.; Ninomiya, T.; Susa, M.; Harris, H. H.; Pickering, I. J.; George, G. N. More on mercury content in fish. *Science* **2004**, *303*, 763b−766b. (c) Korbas, M.; MacDonald, T. C.; Pickering, I. C.; George, G. N.; Krone, P. H. Chemical form matters: differential accumulation of mercury following inorganic and organic mercury exposures in zebrafish larvae. *ACS Chem. Biol.* **2012**, *7*, 411−420.

(9) Mori, N.; Yamamoto, M.; Tsukada, E.; Yokooji, T.; Matsumura, N.; Sasaki, M.; Murakami, T. Comparison of In Vivo with In Vitro Pharmacokinetics of Mercury Between Methylmercury Chloride and Methylmercury Cysteine Using Rats and Caco2 Cells. *Arch. Environ. Contam. Toxicol.* **2012**, *63*, 628−636.

(10) Millow, C. J.; Mackintosh, S. A.; Lewison, R. L.; Dodder, N. G.; Hoh, E. Identifying bioaccumulative halogenated organic compounds using a nontargeted analytical approach: Seabirds as sentinels. *PLoS One* **2015**, *10*, e0127205.

(11) (a) Yin, Y. G.; Li, Y. B.; Tai, C.; Cai, Y.; Jiang, G. B. Fumigant methyl iodide can methylate inorganic mercury species in natural waters. *Nat. Commun.* **2014**, *5*, 4633. (b) Celo, V.; Lean, D. R. S.; Scott, S. L. Abiotic methylation of mercury in the aquatic environment. *Sci. Total Environ.* **2006**, *368*, 126−137.

(12) Riccardi, D.; Guo, H. B.; Parks, J. M.; Gu, B. H.; Summers, A. O.; Miller, S. M.; Liang, L. Y.; Smith, J. C. Why mercury prefers soft ligands. *J. Phys. Chem. Lett.* **2013**, *4*, 2317−2322.

(13) (a) Summers, A. O. Organization, expression, and evolution of genes for mercury resistance. *Annu. Rev. Microbiol.* **1986**, *40*, 607−634. (b) Schottel, J. L. The mercuric and organomercurial detoxifying enzymes from a plasmid-bearing strain of *Escherichia coli*. *J. Biol. Chem.* **1978**, *253*, 4341−4349. (c) Summers, A. O.; Sugarman, L. I. Cell-free mercury (II)-reducing activity in a plasmid-bearing strain of *Escherichia coli*. *J. Bacteriol.* **1974**, *119*, 242−249.

(14) (a) Lafrance-Vanasse, J.; Lefebvre, M.; Lello, P. D.; Sygusch, J.; Omichinski, J. Crystal structures of the organomercurial lyase merb in its free and mercury-bound forms insights into the mechanism of methylmercury degradation. *J. Biol. Chem.* **2009**, *284*, 938−944. (b) Parks, J. M.; Guo, H.; Momany, C.; Liang, L.; Miller, S. M.; Summers, A. O.; Smith, J. C. Mechanism of Hg− C Protonolysis in the Organomercurial Lyase MerB. *J. Am. Chem. Soc.* **2009**, *131*, 13278−13285.

(15) (a) Begley, T.; Walts, A.; Walsh, C. Bacterial organomercurial lyase: overproduction, isolation, and characterization. *Biochemistry* **1986**, *25*, 7186−7192. (b) Begley, T.; Walts, A.; Walsh, C. Mechanistic studies of a protonolytic organomercurial cleaving enzyme: bacterial organomercurial lyase. *Biochemistry* **1986**, *25*, 7192−7200.

(16) (a) Omichinski, J. G. Toward methylmercury bioremediation. *Science* **2007**, *317*, 205−206. (b) Benison, G. C.; Paola, D. L.; Shokes, J. E.; Cosper, N. J.; Scott, R. A.; Legault, P.; Omichinski, J. G. A stable mercury-containing complex of the organomercurial lyase MerB: catalysis, product release, and direct transfer to MerA. *Biochemistry* **2004**, *43*, 8333−8345.

(17) (a) Hong, B.; Nauss, R.; Harwood, I. M.; Miller, S. M. Direct measurement of mercury (II) removal from organomercurial lyase (MerB) by tryptophan fluorescence: NmerA domain of coevolved γ-proteobacterial mercuric ion reductase (MerA) is more efficient than MerA catalytic core or glutathione. *Biochemistry* **2010**, *49*, 8187−8196. (b) Pitts, K. E.; Summers, A. O. The roles of thiols in the bacterial organomercurial lyase (MerB). *Biochemistry* **2002**, *41*, 10287−10296.

(18) Wahba, H. M.; Lecoq, L.; Stevenson, M.; Mansour, A.; Cappadocia, L.; Lafrance-Vanasse, J.; Wilkinson, K. J.; Sygusch, J.; Wilcox, D. E.; Omichinski, J. G. Structural and Biochemical Characterization of a Copper-Binding Mutant of the Organomercurial Lyase MerB: Insight into the Key Role of the Active Site Aspartic Acid in Hg−Carbon Bond Cleavage and Metal Binding Specificity. *Biochemistry* **2016**, *55*, 1070−1081.

(19) Di Lello, P.; Omichinski, J. G.; Lafrance-Vanasse, J. *The organomercurialslyaseMerB*; Wiley: Hoboken, NJ, 2011.

(20) Chien, M. F.; Narita, M.; Lin, K. H.; Matsui, K.; Huang, C. C.; Endo, G. Organomercurials removal by heterogeneous merB genes harboring bacterial strains. *J. Biosci. Bioengin.* **2010**, *110*, 94−98.

(21) (a) Diez-Barra, E.; de la Hoz, A.; Sanchez-Migallon, A.; Tejeda, J. Phase transfer catalysis without solvent: synthesis of bisazolylalkanes. *Heterocycles* **1992**, *34*, 1365−1372. (b) Viciano, M.; Mas Marza, E.; Poyatos, M.; Sanau, M.; Crabtree, R. H.; Peris, E. An N-Heterocyclic Carbene/Iridium Hydride Complex from the Oxidative Addition of a Ferrocenyl−Bisimidazolium Salt: Implications for Synthesis. *Angew. Chem., Int. Ed.* **2005**, *44*, 444−447. (c) Hwang, I.-C.; Chandran, R. P.; Singh, N. J.; Khandelwal, M.; Thangadurai, T. D.; Lee, J.-W.; Chang, J. A.; Kim, K. S. Organic− Inorganic Hybrid Compounds of Li with Bisimidazole Derivatives: Li Ion Binding Study and Topochemical Properties. *Inorg. Chem.* **2006**, *45*, 8062−8069. (d) Claramunt, R. M.; Elguero, J.; Meco, T. N-Polyazolylmethanes. III. Synthesis and proton NMR study of 1,1′-methylenediimidazole and 1,1′-methylenedibenzimidazole derivatives. *J. heterocyclic chem.* **1983**, *20*, 1245−1249. (e) Roy, G.; Jayaram, P. N.; Mugesh, G. *Chem. - Asian J.* **2013**, *8*, 1910−1921.

DOI: 10.1021/acs.inorgchem.7b01048
Inorg. Chem. XXXX, XXX, XXX−XXX

(22) (a) Silva, R. M.; Smith, M. D.; Gardinier, J. R. Unexpected New Chemistry of the Bis (thioimidazolyl) methanes. *J. Org. Chem.* **2005**, *70*, 8755−8763. (b) Bhabak, K. P.; Satheeshkumar, K.; Jayavelu, S.; Mugesh, G. Inhibition of peroxynitrite- and peroxidase-mediated proteintyrosine nitration by imidazole-based thiourea and selenourea derivatives. *Org. Biomol. Chem.* **2011**, *9*, 7343−7350. (c) Williams, D. J.; Vanderveer, D.; Jones, R. L.; Menaldino, D. S. Main group metal halide complexes with sterically hindered thioureas XI. Complexes of antimony (III) and bismuth (III) chlorides with a new bidentate thiourea—1, 1′-methylenebis (3-methyl-2H-imidazole-2-thione). *Inorg. Chim. Acta* **1989**, *165*, 173−178. (d) Meyer, S.; Demeshko, S.; Dechert, S.; Meyer, F. Synthesis, structure and Mössbauer characterization of polymeric iron (II) complexes with bidentate thiourea ligands. *Inorg. Chim. Acta* **2010**, *363*, 3088−3092. (e) Jia, W. G.; Huang, Y. B.; Lin, Y. J.; Jin, G.-X. Syntheses and structures of half-sandwich iridium (III) and rhodium (III) complexes with organo-chalcogen (S, Se) ligands bearing N-methylimidazole and their use as catalysts for norbornene polymerization. *Dalton Trans.* **2008**, *41*, 5612−5620.

(23) (a) Melnick, J. G.; Parkin, G. Cleaving Mercury-Alkyl Bonds: A Functional Model for Mercury Detoxification by *MerB*. *Science* **2007**, *317*, 225−227. (b) Melnick, J. G.; Yurkerwich, K.; Parkin, G. Synthesis, Structure, and Reactivity of Two-Coordinate Mercury Alkyl Compounds with Sulfur Ligands: Relevance to Mercury Detoxification. *Inorg. Chem.* **2009**, *48*, 6763−6772. (c) Melnick, J. G.; Yurkerrwich, K.; Parkin, G. On the Chalcogenophilicity of Mercury: Evidence for a Strong Hg−Se Bond in [Tm^{But}]HgSePh and Its Relevance to the Toxicity of Mercury. *J. Am. Chem. Soc.* **2010**, *132*, 647−655. (d) Sattler, W.; Yurkerwich, K.; Parkin, G. Molecular structures of protonated and mercurated derivatives of thimerosal. *Dalton Trans.* **2009**, 4327−4333. (e) Palmer, J. H.; Parkin, G. 2-Seleno-1-alkylbenzimidazoles and their diselenides: synthesis and structural characterization of a 2-seleno-1-methylbenzimidazole complex of mercury. *Polyhedron* **2013**, *52*, 658−668. (f) Yurkerwich, K.; Quinlivan, P. J.; Rong, Y.; Parkin, G. Phenylselenolate mercury alkyl compounds, PhSeHgMe and PhSeHgEt: Molecular structures, protolytic Hg−C bond cleavage and phenylselenolate exchange. *Polyhedron* **2016**, *103*, 307−314.

(24) Barbaro, P.; Cecconi, F.; Ghilardi, C. A.; Midollini, S.; Orlandini, A.; Vacca, A. Metal coordination and Hg-C bond protonolysis in organomercury (II) compounds. Synthesis, characterization, and reactivity of the tetrahedral complexes [(np3)HgR][$(CF_3)SO_3$]{np3 = N $(CH_2CH_2PPh_2)_3$; R= CH_3, C_2H_5, C_6H_5}. *Inorg. Chem.* **1994**, *33*, 6163−6170.

(25) (a) Chen, J. X.; Zhang, W. H.; Tang, X. Y.; Ren, Z. G.; Zhang, Y.; Lang, J. P. Assembly of a New Family of Mercury (II) Zwitterionic Thiolate Complexes from a Preformed Compound [Hg $(Tab)_2$]$(PF_6)_2$ [Tab= 4-(Trimethylammonio) benzenethiolate]. *Inorg. Chem.* **2006**, *45*, 2568−2580. (b) Tang, X. Y.; Chen, J. X.; Liu, G. F.; Ren, Z. G.; Zhang, Y.; Lang, J. P. Reactions of [$Hg(Tab)_2$]$(PF_6)_2$ [Tab= 4-(trimethylammonio) benzenethiolate] with NaX (X= Cl, NO_2, NO_3): Isolation and Structural Characterization of a Series of Mono-and Binuclear Hg/Tab/X Compounds. *Eur. J. Inorg. Chem.* **2008**, *2008*, 2593−2600. (c) Tang, X. Y.; Yuan, R. X.; Ren, Z. G.; Li, H. X.; Zhang, Y.; Lang, J. P. Interactions of a Cationic Mercury (II) Thiolate Complex [Hg (Tab) 2](PF6) 2 with N-Donor Ligands. *Inorg. Chem.* **2009**, *48*, 2639−2651. (d) Tang, X. Y.; Zheng, A. X.; Shang, H.; Yuan, R. X.; Li, H. X.; Ren, Z. G.; Lang, J. P. Binding of a coordinatively unsaturated mercury (II) thiolate compound by carboxylate anions. *Inorg. Chem.* **2011**, *50*, 503−516. (e) Tang, X. Y.; Yuan, R. X.; Chen, J. X.; Li, H. X.; Zheng, A. X.; Zhao, W.; Ren, Z. G.; Lang, J. P. Group 12 metal zwitterionic thiolate compounds: preparation and structural characterization. *Dalton Trans.* **2012**, *41*, 6162−6172. (f) Zheng, A. X.; Li, H. X.; Hou, K. P.; Shi, J.; Wang, H. F.; Ren, Z. G.; Lang, J. P. Reactions of a methylmercury zwitterionic thiolate complex [MeHg-(Tab)]PF_6 with various donor ligands: relevance to methylmercury detoxification. *Dalton Trans.* **2012**, *41*, 2699−2706. (g) Garoufis, A.; Perlepes, S. P.; Schreiber, A.; Bau, R.; Hadjiliadis, N. Mercury (II)-carbon bond cleavage due to the coordination of the metal by 2-(2′-pyridyl) quinoxaline (L): preparation and characterization of [$Hg_2I_4L_2$] derived from the reaction of CH_3HgI and L. *Polyhedron* **1996**, *15*, 177−182.

(26) Palmer, J. P.; Parkin, G. Protolytic Cleavage of Hg−C Bonds Induced by 1-Methyl-1, 3-dihydro-2 H-benzimidazole-2-selone: Synthesis and Structural Characterization of Mercury Complexes. *J. Am. Chem. Soc.* **2015**, *137*, 4503−4516.

(27) (a) Sens, M. A.; Wilson, N. K.; Ellis, P. D.; Odom, J. D. Mercury-199 fourier transform nuclear magnetic resonance spectroscopy. *J. Magn. Reson.* **1975**, *19*, 323−336. (b) Jokisaari, J.; Raisanen, K. Proton, carbon-13 and mercury-199 NMR studies on dimethyl mercury in isotropic and anisotropic phases. *Mol. Phys.* **1978**, *36*, 113−123.

(28) (a) Banerjee, M.; Karri, R.; Rawat, K. S.; Muthuvel, K.; Pathak, B.; Roy, G. Chemical detoxification of organomercurials. *Angew. Chem.* **2015**, *127*, 9455−9459; *Angew. Chem., Int. Ed.* **2015**, *54*, 9323−9327. (b) Banerjee, M.; Karri, R.; Chalana, A.; Das, R.; Rai, R. K.; Rawat, K. S.; Pathak, B.; Roy, G. Protection of Endogenous Thiols against Methylmercury with Benzimidazole-Based Thione by Unusual Ligand-Exchange Reactions. *Chem. - Eur. J.* **2017**, *23*, 5696−5707.

(29) The ^{199}Hg NMR signal for a standard Ph_2Hg compound (0.1 M) in DMSO-d_6 appears at −813 ppm.

(30) (a) Bark, L. S.; Chadwick, N.; Meth-Cohn, O. The synthesis and ligand properties of N, N′-Polymethylene-bridged imidazole-2-thiones and benzimidazole-2-thiones. *Tetrahedron* **1992**, *48*, 7863−7868. (b) Williams, D. J.; Shilatifard, A.; Vanderveer, D.; Lipscomb, L. A.; Jones, R. L. Main group metal halide complexes with sterically hindered thioureas XIII. Crystallographic study of a unique cross-linked polymeric dichlorolead (II) complex with 1, 1′-methylenebis (3-methyl-2 (3H)-imidazolethione). *Inorg. Chim. Acta* **1992**, *202*, 53−57. (c) Silva, R. M.; Smith, M. D.; Gardinier, J. R. Anion-and Solvent-Directed Assembly in Silver Bis (thioimidazolyl) methane Chemistry and the Silver− Sulfur Interaction. *Inorg. Chem.* **2006**, *45*, 2132−2142. (d) Crossley, I. R.; Hill, A. F.; Humphrey, E. R.; Smith, M. K. A Less Carbocentric View of Agostic Interactions: The Complexes [Rh (η^4-cod){H2A (mt) 2}](A= B, C+; mt= Methimazolyl). *Organometallics* **2006**, *25*, 2242−2247. (e) Maria, L.; Moura, C.; Paulo, A.; Santos, I. C.; Santos, I. Synthesis and structural studies of rhenium(I) tricarbonyl complexes with thione containing chelators. *J. Organomet. Chem.* **2006**, *691*, 4773−4806. (f) Jia, W. G.; Huang, Y. B.; Lin, Y. J.; Wang, G. L.; Jin, G. X. Nickel Complexes and Cobalt Coordination Polymers with Organochalcogen (S, Se) Ligands Bearing an N-Methylimidazole Moiety: Syntheses, Structures, and Properties. *Eur. J. Inorg. Chem.* **2008**, *2008*, 4063−4073. (g) Bigoli, F.; Deplano, P.; Devillanova, F. A.; Lippolis, V.; Mercuri, M. L.; Pellinghelli, M. A.; Trogu, E. F. Synthesis, X-ray and spectroscopic characterization of [SnI_2(mbit)$_2$]$(I_3)_2$·2/3I_2 obtained throught the one-step reaction of mbit·2I2 with tin metal powder (mbit = 1,1′-bis(3-methyl-4-imidazoline-2-thione)methane). *Inorg. Chim. Acta* **1998**, *267*, 115−121. (h) Pinder, T. A.; VanDerveer, D.; Rabinovich, D. Lead (II) in a sulfur-rich environment: Synthesis and molecular structure of the first dinuclear bis (mercaptoimidazolyl) methane complex. *Inorg. Chem. Commun.* **2007**, *10*, 1381−1384. (i) Kimani, M. M.; Watts, D.; Graham, L. A.; Rabinovich, D.; Yap, G. P. A.; Brumaghim, J. L. Dinuclear copper (I) complexes with N-heterocyclic thione and selone ligands: synthesis, characterization, and electrochemical studies. *Dalton Trans.* **2015**, *44*, 16313−16324. (j) Kimblin, C.; Bridgewater, B. M.; Churchill, D. G.; Hascall, T.; Parkin, G. Bis (mercaptoimidazolyl)(pyrazolyl) hydroborato complexes of Zinc, Cadmium, and Cobalt: Structural evidence for the enhanced tendency of Zinc in biological systems to adopt Tetrahedral M [S_4] coordination. *Inorg. Chem.* **2000**, *39*, 4240−4243. (k) Kimblin, C.; Hascall, T.; Parkin, G. Modeling the catalytic site of liver alcohol dehydrogenase: Synthesis and structural characterization of a [Bis (thioimidazolyl)(pyrazolyl) hydroborato] zinc complex,[HB (tim^{Me})$_2$pz]ZnI. *Inorg. Chem.* **1997**, *36*, 5680−5681. (l) Stadelman, B. S.; Kimani, M. M.; Bayse, C. A.; McMillen, C. D.; Brumaghim, J. L. Synthesis, characterization, DFT calculations, and electrochemical comparison of novel iron(II) complexes with thione and selone ligands. *Dalton Trans.* **2016**, *45*, 4697−4711.

DOI: 10.1021/acs.inorgchem.7b01048
Inorg. Chem. XXXX, XXX, XXX−XXX

(31) Alvarez, H. M.; Tran, T. B.; Richter, M. A.; Alyounes, D. M.; Rabinovich, D.; Tanski, J. M.; Krawiec, M. Homoleptic group 12 metal bis (mercaptoimidazolyl) borate complexes M (BmR) 2 (M= Zn, Cd, Hg). *Inorg. Chem.* **2003**, *42*, 2149−2156.
(32) Matsumura, F.; Gotoh, Y.; Boush, G. M. Phenylmercuric acetate: metabolic conversion by microorganisms. *Science* **1971**, *173*, 49−51.
(33) (a) Canty, A. J.; Kishimoto, R. British anti-Lewisite and organomercury poisoning. *Nature* **1975**, *253*, 123−125. (b) Canty, A. J.; Kishimoto, R. Formation of diphenylmercury from phenylmercury (II) amino-acid complexes. *Aust. J. Chem.* **1977**, *30*, 669−674.
(34) Pan-Hou, H. S. K.; Imura, N. Role of hydrogen sulfide in mercury resistance determined by plasmid of Clostridium cochlearium T-2. *Arch. Microbiol.* **1981**, *129*, 49−52.
(35) (a) Marvin-DiPasquale, M.; Agee, J.; McGowan, C.; Oremland, R. S.; Thomas, M.; Krabbenhoft, D.; Glimour, C. C. Methyl-mercury degradation pathways: A comparison among three mercury-impacted ecosystems. *Environ. Sci. Technol.* **2000**, *34*, 4908−4916. (b) Barkay, T.; Miller, S. M.; Summers, A. O. Bacterial mercury resistance from atoms to ecosystems. *FEMS Microbiol. Rev.* **2003**, *27*, 355−384.
(36) (a) Glendinning, K. J.; Macaskie, L. E.; Brown, N. L. Mercury tolerance of thermophilic Bacillus sp. and Ureibacillus sp. *Biotechnol. Lett.* **2005**, *27*, 1657−1662. (b) Essa, M.; Macaskie, L. E.; Brown, N. L. A new method for mercury removal. *Biotechnol. Lett.* **2005**, *27*, 1649−1655. (c) Essa, A. M. M.; Creamer, N. J.; Brown, N. L.; Macaskie, L. E. A new approach to the remediation of heavy metal liquid wastes via off-gases produced by Klebsiella pneumoniae M426. *Biotechnol. Bioeng.* **2006**, *95*, 574−576. (d) Macaskie, L. E.; Creamer, N. J.; Essa, A. M. M.; Brown, N. L. A new approach for the recovery of precious metals from solution and from leachates derived from electronic scrap. *Biotechnol. Bioeng.* **2007**, *96*, 631−639.
(37) Baldi, F.; Pepi, M.; Filippelli, M. Methylmercury resistance in Desulfovibrio desulfuricans strains in relation to methylmercury degradation. *Appl. Environ. Microbiol.* **1993**, *59*, 2479−2485.
(38) (a) Craig, P. J.; Barlett, P. D. The role of hydrogen sulphide in environmental transport of mercury. *Nature* **1978**, *275*, 635−637. (b) Rowland, I. R.; Davies, M. J.; Grasso, P. Volatilisation of methylmercuric chloride by hydrogen sulphide. *Nature* **1977**, *265*, 718−719. (c) Khan, M. A.; Wang, F. Chemical demethylation of methylmercury by selenoamino acids. *Chem. Res. Toxicol.* **2010**, *23*, 1202−1206. (d) Asaduzzaman, A. M.; Schreckenbach, G. Degradation mechanism of methyl mercury selenoamino acid complexes: a computational study. *Inorg. Chem.* **2011**, *50*, 2366−2372. (e) Black, F. J.; Conaway, C. H.; Flegal, A. R. Stability of dimethyl mercury in seawater and its conversion to monomethyl mercury. *Environ. Sci. Technol.* **2009**, *43*, 4056−4062. (f) Barone, V.; Bencini, A.; Totti, F.; Uytterhoeven, M. G. Theoretical Characterization of the Mechanism of Hg−C Bond Cleavage by Halogenic Acids. *Organometallics* **1996**, *15*, 1465−1469.
(39) Jonsson, S.; Mazrui, N. M.; Mason, R. P. Dimethylmercury formation mediated by inorganic and organic reduced sulfur surfaces. *Sci. Rep.* **2016**, *6*, 27958.
(40) Electron-donating ligands, $[S_2]$-donor ligands, facilitate the degradation of Me_2Hg in acidic medium.
(41) (a) Dessy, R. E.; Lee, Y. K. The Mechanism of the Reaction of Mercuric Halides with Dialkyl and Diarylmercury Compounds. *J. Am. Chem. Soc.* **1960**, *82*, 689−693. (b) Dessy, R. E.; Lee, Y. K.; Kim, J.-Y. The Mechanism of the Reaction of Mercuric Iodide with Bis-organomercury Compounds. *J. Am. Chem. Soc.* **1961**, *83*, 1163−1167. (c) Rausch, M. D.; Van Wezer, J. R. Exchange reactions and nuclear magnetic resonance analysis of some organomercury compounds. *Inorg. Chem.* **1964**, *3*, 761−764. (d) Murrell, L. L.; Brown, T. L. Organometallic exchange reactions VIII. Exchanges in mixtures of methylmercury halides and pseudohalides. *J. Organomet. Chem.* **1968**, *13*, 301−311.
(42) (a) Canty, A. J.; Marker, A.; Barron, P.; Healy, P. C. A. ^{199}Hg NMR spectroscopic study of two and three-coordinate methylmercury (II) complexes,$[MeHgL]NO_3$. *J. Organomet. Chem.* **1978**, *144*, 371−379. (b) Bach, R. D.; Weibel, A. T. Nuclear magnetic resonance studies on anion-exchange reactions of alkylmercury mercaptides. *J. Am. Chem. Soc.* **1976**, *98*, 6241−6249.
(43) Taylor, R. E.; Gabbaï, F. P. ^{19} F and ^{199} Hg NMR of trimeric perfluoro-*ortho*-phenylenemercury. *J. Mol. Struct.* **2007**, *839*, 28−32.
(44) Crystallographic data of all the crystal structures mentioned in this paper (CCDC 1534008, CCDC 1534011, CCDC 1534012, CCDC 1534014, CCDC 1534015, and CCDC 1544311) can be obtained free of charge from The Cambridge Crystallographic Data Centre (CCDC) via www.ccdc.cam.ac.uk/data_request/cif.
(45) *Bruker Support APEX3, SAINT and SADABS: Software for data reduction, absorption correction and structure solution*; Bruker AXS Inc., Madison, WI, USA, 2015; http://www.brukersupport.com/.
(46) Sheldrick, G. M. *SHELXTL Version 2014/7: Programs for the determination of small and macromolecular crystal structures by single crystal X-ray and neutron diffraction*; University of Göttingen, Göttingen, Germany, 2014; http://shelx.uni-ac.gwdg.de/SHELX/index.php.
(47) Sheldrick, G. M. A short history of *SHELX*. *Acta Crystallogr., Sect. A: Found. Crystallogr.* **2008**, *64*, 112−122.
(48) Farrugia, L. J. ORTEP-3 for Windows - a version of ORTEP-III with a Graphical User Interface (GUI). *J. Appl. Crystallogr.* **1997**, *30*, 565.
(49) Macrae, C. F.; Bruno, I. J.; Chisholm, J. A.; Edgington, P. R.; McCabe, P.; Pidcock, E.; Rodriguez-Monge, L.; Taylor, R.; Streek, J. V.; Wood, P. A. Mercury CSD 2.0 - New Features for the Visualization and Investigation of Crystal Structures. *J. Appl. Crystallogr.* **2006**, *39*, 453−457.
(50) Muller, P.; Herbst-Irmer, R.; Spek, A. L.; Schneider, T. R.; Sawaya, M. R. *Crystal Structure Refinement*; Oxford University Press: Oxford, U.K., 2006.
(51) Spek, A. L. Single-crystal structure validation with the program PLATON. *J. Appl. Crystallogr.* **2003**, *36*, 7.
(52) Frisch, M. J., et al. *Gaussian 09, Revision B.01*; Gaussian Inc., Wallingford, CT, 2009. The full citation is given in the Supporting Information.
(53) Figgen, D.; Rauhat, G.; Dolg, M.; Stoll, H. Energy-consistent pseudopotentials for group 11 and 12 atoms: adjustment to multi-configuration Dirac−Hartree−Fock data. *Chem. Phys.* **2005**, *311*, 227−244.
(54) Glendening, E. D.; Reed, A. E.; Carpenter, J. E.; Weinhold, F. *NBO, version 3.1*; University of Wisconsin, Madison, WI.

DOI: 10.1021/acs.inorgchem.7b01048
Inorg. Chem. XXXX, XXX, XXX−XXX